ZEUS-note 96-132
December 1996

Measurement of F_2^{ep} from the 1995 shifted vertex data

Mirko Raso
Università "La Sapienza" and INFN, Roma, Italy.

Abstract

A measurement of the proton structure function F_2^{ep} has been performed, using the 236 nb^{-1} of shifted vertex e^+p collisions collected in 1995. The kinematical region of this measurement ($10^{-5} < x < 10^{-3}$ and $0.6 < Q^2 < 8.5$ GeV^2) is extended, with respect to the 1994 measurement, down to $Q^2 = 0.6$ GeV^2; thus filling the gap between the BPC and the "nominal vertex" results. An estimate of the total photoproduction cross section has also been performed.

1 Introduction

During 1995, HERA collided 27.5 GeV positrons on 820 GeV protons. ZEUS has collected 7.3 pb^{-1} with the nominal vertex interaction and 236 nb^{-1} with the vertex interaction shifted in the "forward" direction.

This note reports on the measurement of the proton structure function F_2 from the shifted vertex data. The new beam pipe configuration in the "rear" direction gave the possibility to measure at lower Q^2, compared to 1994 data; the kinematical range is extended in Q^2 down to 0.6 GeV^2 and in x down to 10^{-5}.

Most of the offline cuts used in this analysis are the same of '94 analysis [1]. Using the experience of our previous results, the SRTD was used for the positron reconstruction and to provide positron energy correction. The *electron method* was used to reconstruct the kinematical variables. The analysis was carried out using the Bayesian unfolding which gives the possibility to include correlation effects. Moreover, to estimate the uncertainties due to

the systematic errors a Bayesian approach has also been used, in agreement with BIPM and ISO recommendation [2].

This note is structured in the following way: section 2 describes the used Monte Carlo samples, while section 3 describes the data and the selection cuts. In section 4 the unfolding procedure and F_2 extraction method are presented. The systematic sources are treated in section 5 and, finally, section 6 presents the obtained results.

2 Monte Carlo simulation

The Monte Carlo sample used for this analysis has been generated using DJANGO6.1 [3] with HERACLES 4.4 [4] for QED correction, LEPTO 6.1 [5] and ARIADNE 4.06 [6] for lepton-nucleon scattering simulation and hadronization. The Monte Carlo samples consist of:

- $Q^2 > 0.1$ GeV^2, MRSA structure function, corresponding to a luminosity of 14.3 nb^{-1} (15 K events).
- $Q^2 > 0.3$ GeV^2 and $y > 0.033$, MRSA [7] structure function, corresponding to a luminosity of 14.2 nb^{-1} (60 k events).
- $Q^2 > 0.5$ GeV^2, MRSA structure function, corresponding to a luminosity of 43.5 nb^{-1} (150 k events).
- $Q^2 > 0.5$ GeV^2, MRSA structure function, corresponding to a luminosity of 2.9 nb^{-1} (10 K events) with the vertex at $z = +136$ cm.
- $Q^2 > 0.3$ GeV^2, ZEUS 94 [1] structure function, corresponding to a luminosity of 229 nb^{-1} (720 k events).
- $Q^2 > 0.3$ GeV^2 and $y > 0.033$, ZEUS 94 structure function, corresponding to a luminosity of 241 nb^{-1} (390 k events).

For ZEUS 94 parametrization F_L was set to zero. The MC sample with $Q^2 > 0.1$ GeV^2 has been used to take into account the migration in the low Q^2 region. The MC events with the vertex at $z = +136$ cm were used due to the wrong simulation of the vertex distribution in that region. To simulate the detector's response the num95v1.1 funnel version has been used.

3 Event Selection and reconstruction of the kinematical variables

The data collected for this analysis correspond to 236 nb^{-1} of positron-proton collisions. The DIS events are firstly selected online by the three level trigger logics [8]. Most of the offline cuts used in this analysis are the same used in the 1994 analysis [1]. The same selection criteria are applied both to data and Monte Carlo except for the *timing*, due to its wrong simulation. The kinematical variables are extracted using the *electron method*. Some checks were performed in order to see if the detector response is well simulated.

3.1 Energy measurement

In 1994 the scattered positron energy was corrected using the SRTD. Due to the changes in the rear part of the detector, the '94 energy correction function has been checked. The procedure is the same described in [9], but only the kinematical peak events ($Q^2 < 100$ GeV^2 and $y_{JB} < 0.03$) for all '95 shifted vertex data and for a sample of '95 nominal vertex data (corresponding to the luminosity of 118 nb^{-1}) has been used for this test (the '94 correction function was calculated using a sample of nominal vertex data).

Figure 1 shows the comparison between data (dots) and '94 correction function (solid line) for both sample of data (shifted and nominal vertex). For the nominal vertex there is a good agreement between data and the correction function while, in the shifted vertex case, a discrepancy of the order of 2-3%, at high MIPs, is shown. There is however a good agreement, as shown in figure 2a, for the energy distribution of the kinematical peak events between data and Monte Carlo.

As suggested by J.T. Wu, a new fit (dotted line) of the energy correction function was done just changing only one parameter. In this analysis, the new correction function has been used only as an additional systematic check.

No correction was applied to the hadronic energy, but the $(p_t^{el} - p_t^{had})$ distribution seems to be described by the Monte Carlo with a sufficient accuracy, even if a shift between data and Monte Carlo of the order of 8% is present. Some recent studies have shown a possible miscalibration of the calorimeter (5% in BCAL and 2.5% in RCAL). Anyway, these effects will be taken into account in the systematics' studies.

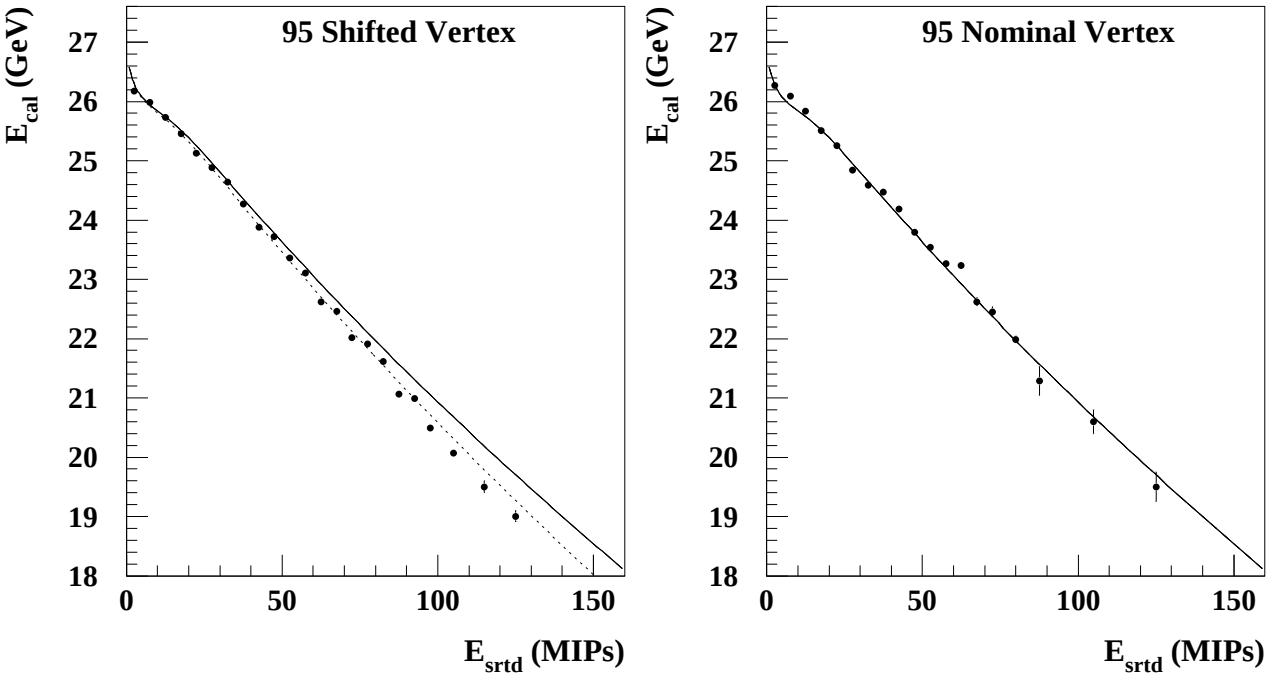

Figure 1: *Comparison '95 data (dots) with '94 energy correction function (solid line). The new energy correction function (dotted line) is shown, too.*

3.2 Positron angle measurement

The positron angle is obtained as the ratio of the position on the transverse plane and the distance on the z axis between the interaction and impact point. So, to check this measurement, it is sufficient to check the measurement of the impact position and of the vertex position.

- *Impact position*

  The position of the data was shifted of the right amount to take into account the shift of the RCAL/SRTD compared to track system. In fact it was found [10] a shift of -3(-1) mm in $x(y)$ for the right side and -1(+2) mm in $x(y)$ for the left side. In 1995 the RCAL module 12 was put at 4 cm in y, instead of 10, from the beam pipe. In order to see which is the best choose for the new "box cut" a sample of KP events with an energy, in the SRTD, between 0 and 5 MIPs, have been used. In this way a sample of events with almost constant energy was selected. In figure 3 the dependence of the energy from the impact point in y is shown. The scattered positron seems to be well contained

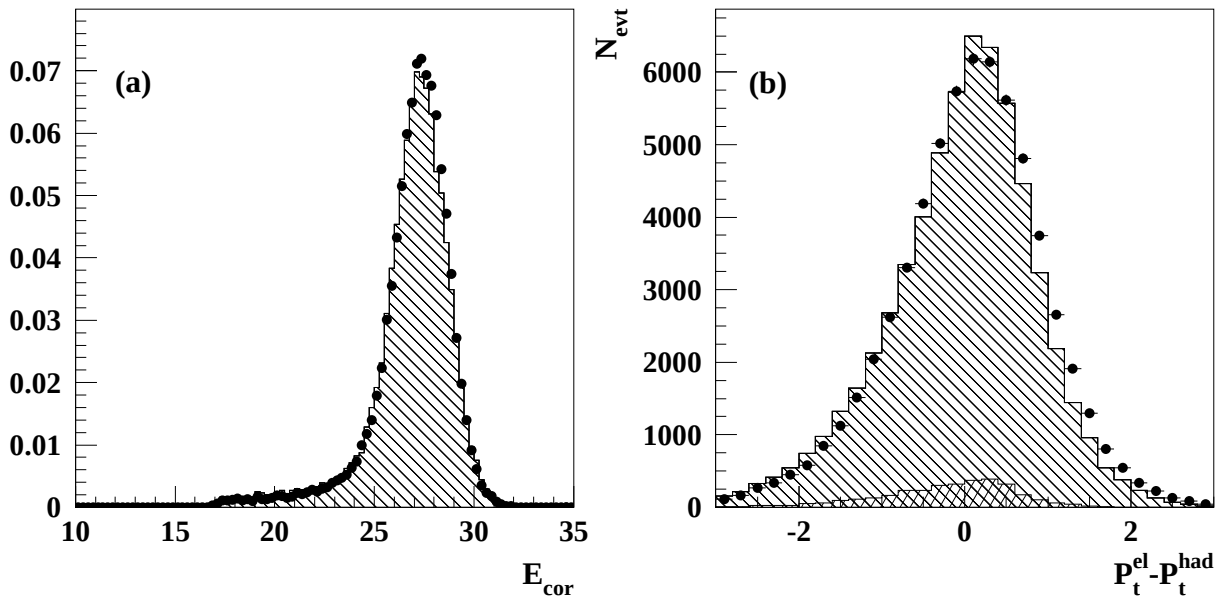

Figure 2: *a) Energy distribution of kinematical peak events for data (dots) and Monte Carlo (hatched histogram). b)* $p_t^{el} - p_t^{had}$ *for data (dots) and Monte Carlo.*

in the calorimeter above 8 cm. In figure 3 is also shown the dependence from the impact point on x direction. For this check the energy in the SRTD was between 30 and 35 MIPs. In x direction a cut at 13 cm is required.

- *Vertex distribution*

  The primary z vertex position is measured by the tracking. For event with no track the vertex is set to the nominal interaction point that means $z = +70$ cm. The z distribution is shown in figure 4.

  The central peak is well reproduced. Unfortunately this is not the case for the peak given by the events in the satellite bunches, and for the events without a measured vertex. The efficiency, given by the ratio of events with a tracking vertex and all events, for the events with an hadronic angle $\gamma_H \sim 30^o$ is around 50% while for $\gamma_H > 80^o$ is greater than 90%. In order to have a better description of the events in the satellites, a limited sample (corresponding to a luminosity of 2.9 nb^{-1}) with the vertex at $z = +136$ cm was used. To use in the

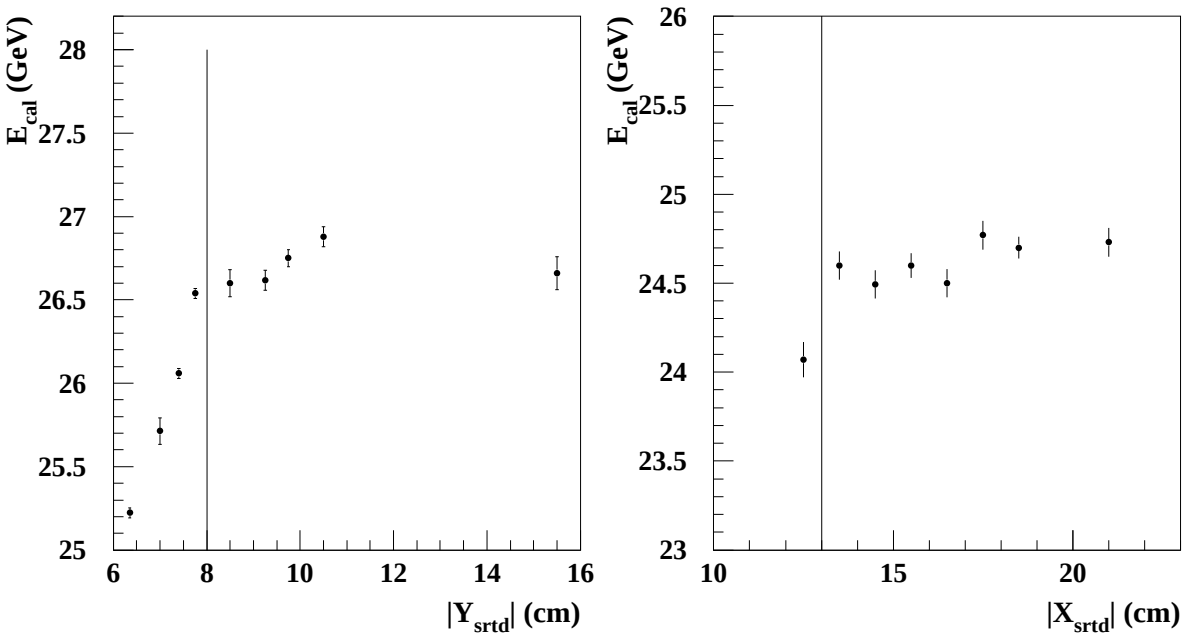

Figure 3: *Energy dependence from the impact point in y and x direction. The vertical solid lines represent the cuts used in this analysis.*

best way the different resolution for the different approaches to obtain the vertex, two different analysis should be implemented (one for the events with a vertex and another one for the events without a track) and then the results should be combined. But the limited statistics gives no possibility to do it. However an analysis was done using only the events with a reconstructed vertex and no significance (less than 2%) deviations were registered. These effects will be taken into account in the systematics' studies.

3.3 Trigger

At the first level trigger (FLT) the energy deposits in BCAL and RCAL are checked. So it is required an .OR. of the following triggers:

Remc This trigger sums the energy deposits from the entire RCAL EMC-section excluding the towers around the beam hole. The energy deposit has to be greater than 3.4 GeV.

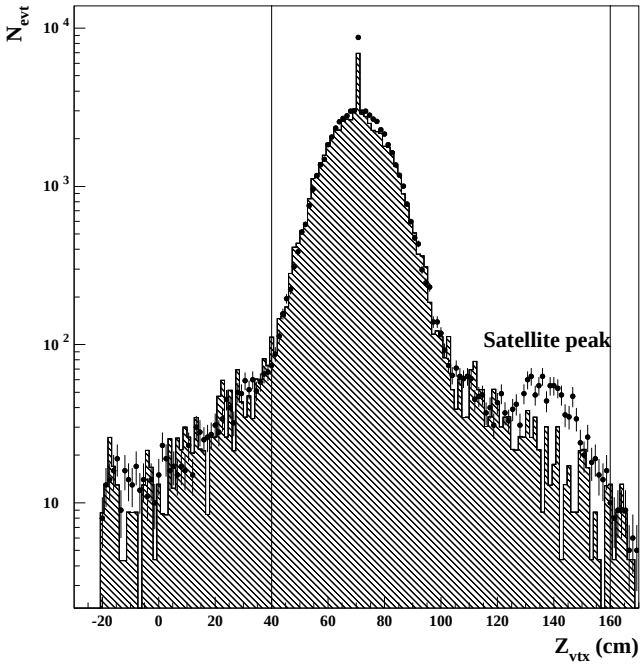

Figure 4: *Comparison data (dots) and Monte Carlo (histogram) for the z vertex distribution. The solid lines represent the applied cuts.*

Bemc This trigger sums the energy deposits from the entire BCAL EMC-section. The energy deposit has to be greater than 4.8 GeV.

Remc-th This trigger sums the energy deposits from the entire RCAL EMC-section including the towers around the beam hole. The energy deposit has to be greater than 3.75 GeV.

IsoE This trigger requires an isolated lepton in the RCAL. This trigger was put in coincidence with **Remc-th**, due to its high rate. The efficiency of this trigger is greater than 99%, after all cuts.

At the second level (SLT), in addition to the global vetoes (timing, spark rejection,etc.), an $E - P_z$ cut of 29 GeV is required.
At the third level (TLT) a positron with a box cut of $12(x)\times6(y)$ cm with an energy greater than 4 GeV is required. In addition $E - P_z + 2E_\gamma > 30$ GeV and $E - P_z < 100$ GeV.

To summarize, the following selection cuts were applied:

- *Positron identification*:

  The analysis was done requiring a positron with **siNISTra95** with a probability cut of 0.9.

- *Positron Energy*:

  The scattered positron energy $E'_e > 10$ GeV and the probability of siNISTra associated to the candidate $Pro > 0.9$ were required. This cut ensures an high efficiency and purity to find the scattered positron by the electron finder and reduces the photoproduction (PHP) contribution.

- *Positron position*:

  The impact point of the positron on the RCAL face was reconstructed using the SRTD. So it is required that the positron is found in the region $|x+1| < 32$ cm, $|y| < 26$ cm. Events where the positron was not properly reconstructed by the SRTD were excluded, otherwise a "box cut" $|x| > 13$.OR.$|y| > 8$ cm was applied. In addition positrons 1 cm away from the two SRTD gaps were excluded.

- $E - P_z$:

  This cut reduces the hard initial state radiation events and the *e-gas* and PHP backgrounds, too.

  So it was required that 35 GeV $< E - P_z <$ 65 GeV.

- y_{JB}:

  In order to reduce the uranium noise a y_{JB} cut at 0.04 was applied. Because of the *electron method* is used, this cut gives also a better resolution for the reconstruction of the kinematical variables.

- *Interaction Vertex*:

  If a vertex is found, the z component of the vertex is required to be in the range $40 < Z_{vtx} < 160$ cm. For the events without a reconstructed vertex, it is put at $z = +70$ cm.

- *timing*:

  This cut was applied only to the data. The event time of data was corrected using C5 counter. The following cuts were used:

$$|t_{RCAL}| < 6 \text{ ns} \qquad |t_{RCAL} - t_{FCAL}| < 6\text{ns} \tag{1}$$

- *Trigger*:

  The trigger conditions, described above, were selected requiring the bit 20.

- *Cosmic and halo μ rejection*:

  This background is rejected using the ALHALO2, MUFLAG and ISITAMU routine.

The total of 64 k events were left after these cuts.

3.4 Background

After applying the selection cuts, the background is still present in the data.

The main background is due to photoproduction events (PHP). This source of background was estimated using the PYTHIA Monte Carlo simulation [11].

For this analysis a sample corresponding to 211 nb^{-1} was used. The contribution of PHP MC events varies from 1% in the low y bins, to 25% in the highest y bins.

The contribution of the *e-gas* and *p-gas* background was evaluated counting the number of events in the *e-pilot* and *p-pilot* bunches that pass the selection cuts. The *p-gas* background varies from 3% at high y to 5% in the low y bins. For *e-gas*, the contribution is less than 2% in low y bins and less than 1% in the high y bins.

The contribution of cosmic ray was estimated looking at the events in the empty bunches that pass the selection cuts. No event was found. So, if λ is the expected number of events and x is the measured number of events, using the Bayes' theorem, the density distribution of probability, for λ, is:

$$f(\lambda|x) \sim \frac{\lambda^x e^{-\lambda}}{x!} f_o(\lambda) \tag{2}$$

Assuming a uniform distribution for f_o, the expected value and variance are $E[\lambda] = x + 1$ and $Var(\lambda) = x + 2$, respectively. In this analysis $x = 0$ so the expected value is 1 with the variance 2 and a 95% upper limit of 3; so it is possible to neglect the cosmic contribution because the measured number of events are around 64 k.

In this analysis the contribution of background is not subtracted statistically but it is included directly in the unfolding procedure, which will be described in the next section.

3.5 Reconstruction

The *Electron method* was used to reconstruct the kinematical variables. Figure 5 and 6 show a comparison of data and Monte Carlo after cuts. The distribution in the Monte Carlo are normalized to the luminosity in the data. For these plots the MRSA events were weighted to ZEUS NLO 94 ($F_L \neq 0$) [12], and the ZEUS 94 MC events were weighted to ZEUS NLO 94 with $F_L \neq 0$. Only MRSA with $Q^2_{app} > 0.3$ GeV^2 have been used and a cut at $z = 100$ cm was applied (in the analysis it is at 160 cm).

From figure 5 appears that the positron energy distribution is well described by Monte Carlo. There is a very good agreement between data and Monte Carlo for the positron angle distribution; this means that the SRTD/CAL misalignment is under control. Also the hadronic angle distribution is well reproduced. There is an excess in the Monte Carlo in the region of high y for the y_{JB} distribution and this effect is reflected in the $E - P_z$ distribution.

Looking at the x_{el}, y_{el} and Q^2_{el} distributions, a very good agreement is found. In addition also the kinematical variables given by the *double angle method* (DA) are reported. In this way it is possible to compare the different resolution in different phase space regions for these two reconstruction methods.

To summarize, the Monte Carlo simulation describes the data with a good approximation. The absence of a good description of dead material gives some problem especially for the hadronic variables.

4 Extraction of F_2 and unfolding procedure

The structure function F_2 was extracted using the Bayesian unfolding described in [13]. F_2 is directly extracted from the measured number of events, through the measurement of the differential cross section. In the next subsections the bin selection criteria, how F_2 is extracted and the used unfolding procedure will be described.

4.1 Bin selection criteria

In order to have a best cover of the phase space, a binning in y and Q^2 was chosen. Figure 7 shows the (x, Q^2) distribution with the bins used in this analysis. There are 9 bins in Q^2 and 5 in x except for the low Q^2 bins, where there are only 1 and 3 bins for $Q^2 = 0.6$ GeV^2 and $Q^2 = 0.85$ GeV^2, respectively.

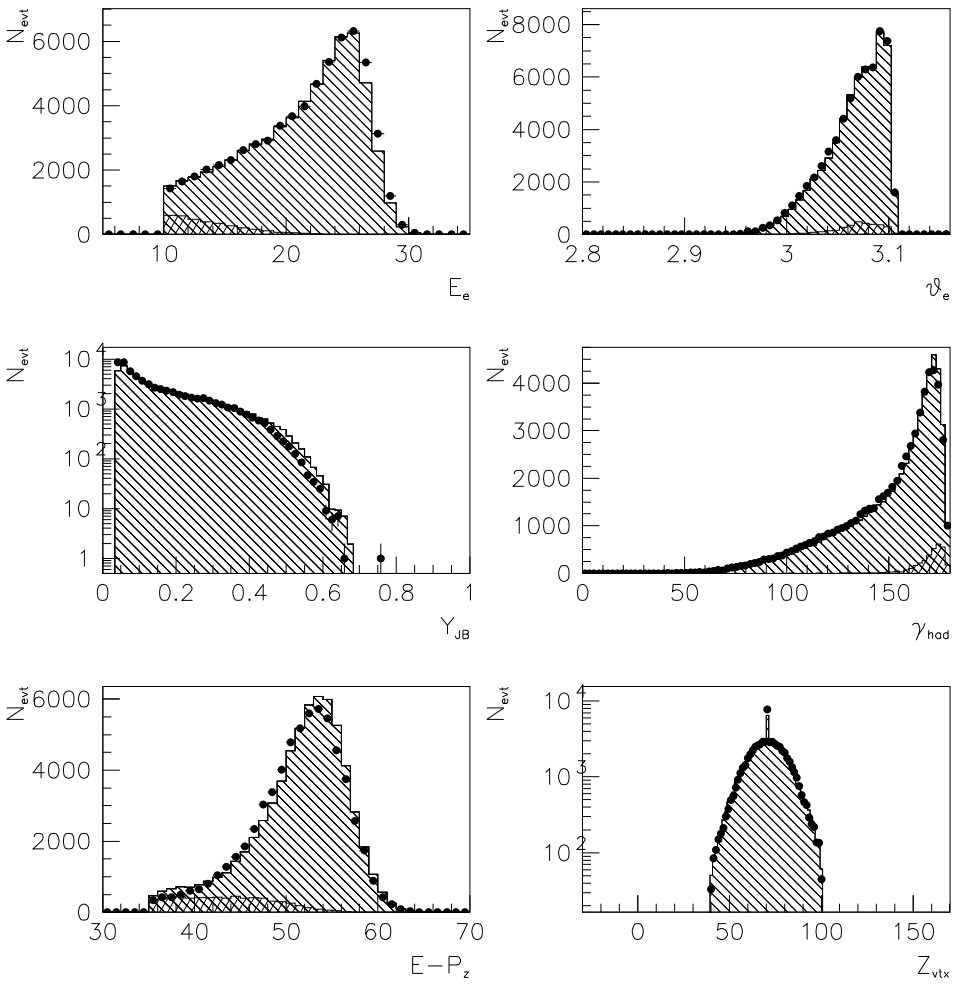

Figure 5: *Comparison Data (dots) and Monte Carlo (histogram) for the positron energy, positron polar angle, vertex distribution, hadronic angle and y_{JB}. The PHP background is shown as double hatched histogram.*

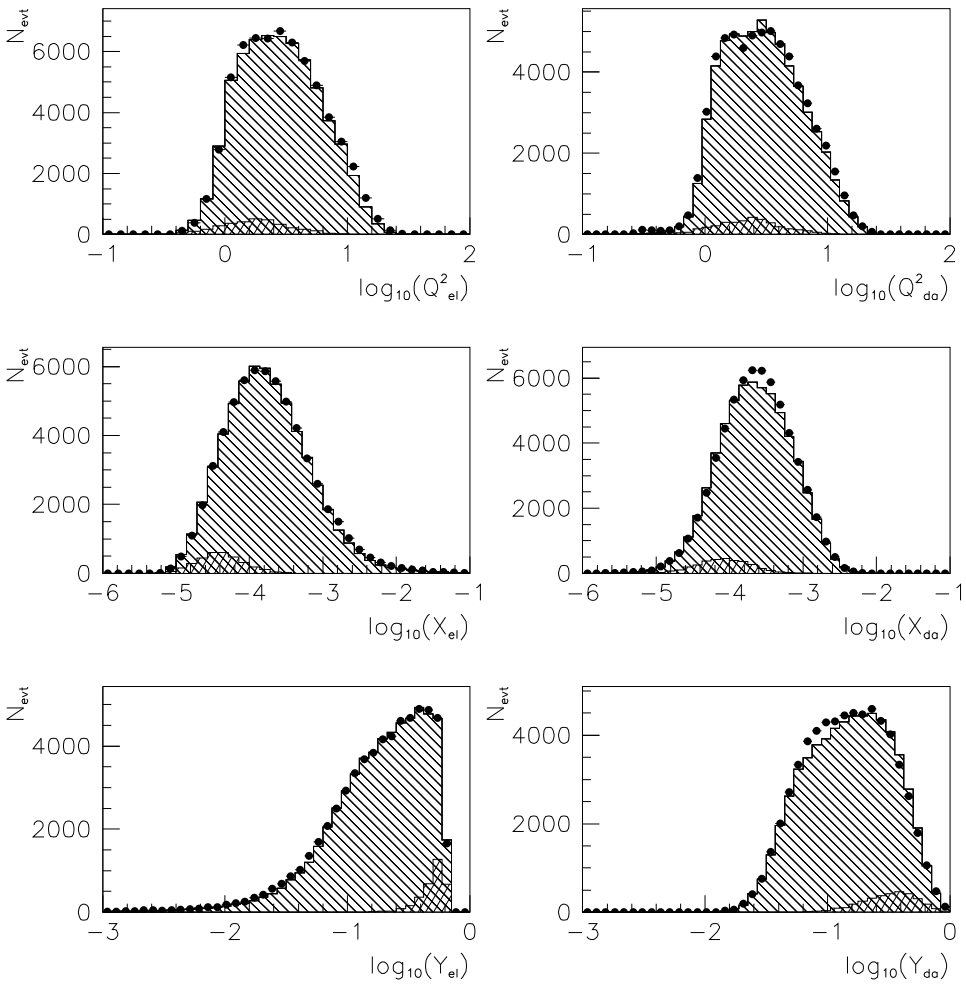

Figure 6: *Comparison data (dots) and Monte Carlo (histogram) for the kinematical variables Q^2, y and x for the electron method. The same kinematical variables are also shown for the Double Angle method. The PHP background is shown as double hatched histogram.*

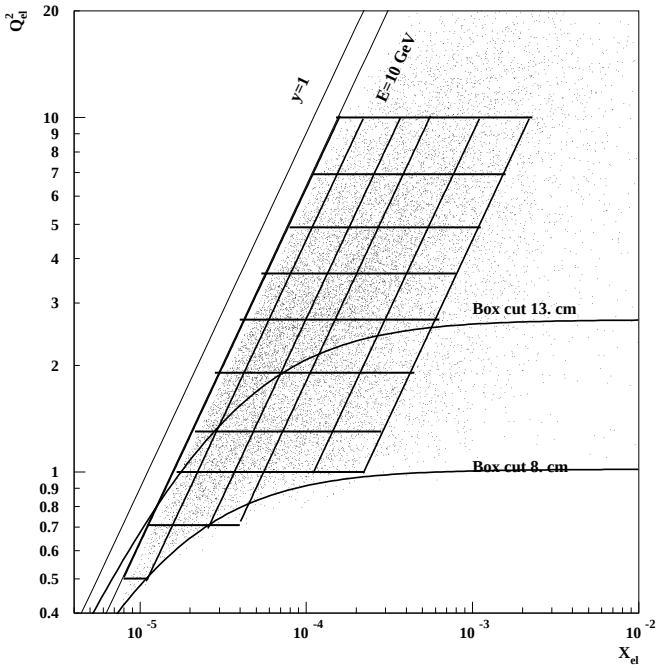

Figure 7: *Events distribution in the (x,Q^2) plane. The bins used in the analysis are shown together with the lower limit given by the new beam pipe.*

Due to the detector resolution the bins are correlated. In fact it is possible to reconstruct in the bin j an event E, generated in the bin i. The probability $P(E|C_i)$ to find the event E in a different bin is as high as the resolution is poor. The poor resolution of the detector is not a problem if the probability $P(E|C_i)$ is well known. In a realistic situation the knowledge is imperfect (but not zero) and the bins were chosen in a such a way that the correlations are contained at the first neighbours. The resolution (horizontal and vertical lines) and the migration (arrow) for each bin are shown in figure 8. At low Q^2 there is an high migration towards high values, essentially due to the initial state radiation. In y the migrations are well contained. Fitting with a gaussian the following variables,

$$Q^2_{res} = \frac{Q^2_v - Q^2_{el}}{Q^2_v} \quad (3)$$

$$y_{res} = \frac{y_v - y_{el}}{y_v} \quad (4)$$

$\sigma(Q^2_{res})$ and $\sigma(y_{res})$ give an estimate of the resolution for the kinematical

variables in each bin. Horizontal line represents the value $y_o \pm \sigma$, while vertical line is $Q_o^2 \pm \sigma$, with σ given by the fit. Q_o^2 and y_o represent the center of the bin in Q^2 and y. Except for the low y bin, all the bins are well defined also in terms of resolution.

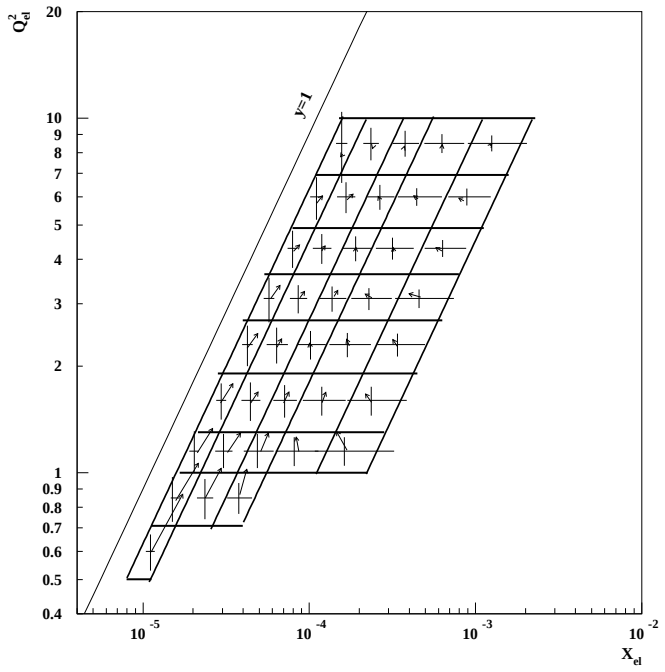

Figure 8: *The resolution (vertical and horizontal line) and the migration (arrow) for each bin are shown. The starting point of the arrow is the average value of the generated events in the bin; the final point is the average value of the reconstructed event.*

4.2 Measurement of the differential cross section

The structure function F_2 is obtained by the measurement of the differential cross section, which is in fact the empirical observable. The number of events in a bin is given by the integrated luminosity L times the total cross section in the bin.

$$N_{evt} = L \int\int_{bin} dy\ dQ^2 \left(\frac{d^2\sigma}{dydQ^2} \right). \tag{5}$$

If (y_o, Q_o^2) is the center of the bin, the differential cross section can be expanded in Taylor's series around this point. Taking into account up to the

second order terms, we obtain:

$$f(y,Q^2) = f(y_o,Q^2_o) + \frac{\partial f}{\partial y}(y-y_o) + \frac{\partial f}{\partial Q^2}(Q^2-Q^2_o) + \frac{1}{2}\frac{\partial^2 f}{\partial y^2}(y-y_o)^2 + \frac{1}{2}\frac{\partial^2 f}{\partial Q^4}(Q^2-Q^2_o)^2 + \frac{\partial^2 f}{\partial y \partial Q^2}(y-y_o)(Q^2-Q^2_o) \quad (6)$$

where $f(y,Q^2) \equiv \frac{d^2\sigma}{dy\,dQ^2}$. Calling Δy and ΔQ^2 the widths of the bin in y and Q^2, we get:

$$\frac{N_{evt}}{L} = f(y_o,Q^2_o)\Delta y \Delta Q^2 + \frac{1}{24}\frac{\partial^2 f}{\partial y^2}\Delta Q^2(\Delta y)^3 + \frac{1}{24}\frac{\partial^2 f}{\partial Q^4}\Delta y(\Delta Q^2)^3 \ . \quad (7)$$

The second order terms take into account the non-linearity effects. In order to estimate these values, a two-steps procedure is used. As first step, we can consider negligible the second order terms respect to the first one, so equation (7) becomes

$$f_o \equiv f(y_o,Q^2_o) = \frac{N_{evt}}{L\Delta y \Delta Q^2} \ . \quad (8)$$

Once that f_o's are known, it is possible to compute the second order terms, as seen as correction factors to the zero-th order. To compute these factors, we need to know the derivative respect to Q^2 and y at fixed y and Q^2, respectively. An easy way to get these values is to find an analytical function to fit the f_o distribution and so, simply deriving this function, the second order terms are calculated. In figure 9 the behaviour at fixed Q^2 is reported, while in figure 10 the one at fixed y. The curves, given by the fit, are also shown.

The "ad hoc" analytical function used for both case (fixed y or Q^2) is

$$f(z) = \frac{N}{z^\alpha}e^{-\beta z} \ , \quad (9)$$

where z is y or Q^2, and N is a normalization factor.

For fixed y ($z = Q^2$), α changes from 1.4 e 1.8 while β is between 0.001 and 0.1.

For fixed Q^2 ($z = y$), α is between 0.9 and 1.1 and β is between 0.4 and 0.6.

Knowing the second order terms, the differential cross section in (y_o, Q^2_o) will be given by the following formula:

$$\frac{d^2\sigma}{dy\,dQ^2} \equiv f(y_o,Q^2_o) = \frac{N_{evt}}{L\Delta y \Delta Q^2} - \frac{1}{24}\left[(\Delta y)^2\frac{\partial^2 f}{\partial y^2} + (\Delta Q^2)^2\frac{\partial^2 f}{\partial Q^4}\right] \ . \quad (10)$$

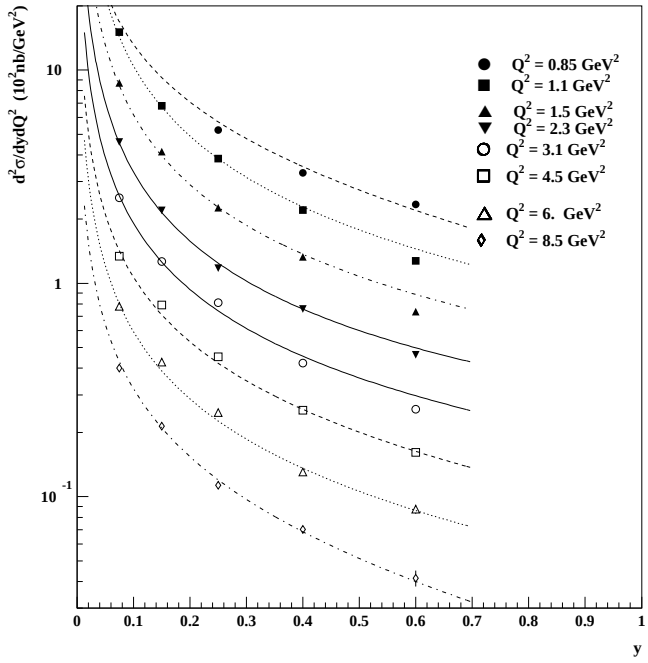

Figure 9: *Behaviour of the differential cross section in y with fixed Q^2. The curves show an analytical "ad hoc" parametrization (see text).*

4.3 Extraction of F_2

The cross section is related to the structure functions F_2, F_L and F_3 by

$$\frac{d^2\sigma}{dydQ^2} = \frac{2\pi\alpha^2}{yQ^4} Y_+ \underbrace{\left[F_2(y,Q^2) - \frac{y^2}{Y_+} F_L(y,Q^2) - \frac{Y_-}{Y_+} x F_3(y,Q^2) \right]}_{\tilde{F}_2} \qquad (11)$$

where $Y_\pm = 1 \pm (1-y)^2$. The quantity $\tilde{\mathrm{F}}_2$, given by

$$\tilde{F}_2(x_o, Q_o^2) = \frac{y_o Q_o^4}{2\pi\alpha^2 Y_+} \left(\frac{N_{evt}}{L\Delta y \Delta Q^2} - \frac{1}{24} \left[(\Delta y)^2 \frac{\partial^2 f}{\partial y^2} + (\Delta Q^2)^2 \frac{\partial^2 f}{\partial Q^4} \right] \right) \ , \qquad (12)$$

depends on the differential cross section alone. In order to obtain F_2, it is helpful to explicit the F_L contribution (xF_3 is negligible in the low Q^2 region) in this way:

$$F_2 = r\tilde{F}_2 \ , \qquad (13)$$

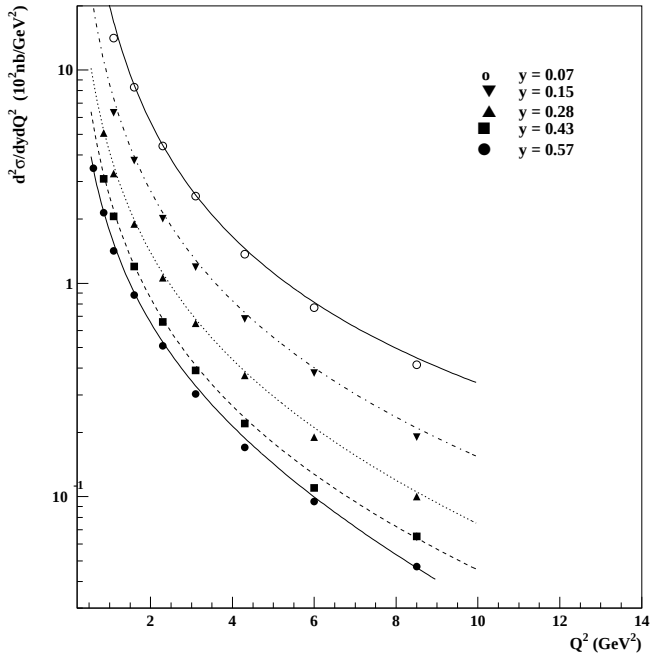

Figure 10: *Behaviour of the differential cross section in Q^2 with fixed y. The curves show an analytical "ad hoc" parametrization (see text).*

where

$$r = \frac{F_2}{F_2 - \frac{y^2}{Y_+} F_L} = \frac{1}{1 - \frac{y^2}{Y_+}\frac{F_L}{F_2}} \sim \left(1 + \frac{y^2}{Y_+}\frac{F_L}{F_2}\right) \ . \tag{14}$$

The r value has been calculated with ZEUS NLO fit to '94 data and it lays in the range between 1. and 1.06. For the bin at $Q^2 = 0.6$ GeV^2, F_L was set at zero.

4.4 Unfolding implementation

A Bayesian unfolding [15]has been used. As every unfolding technique, it relies on the detailed knowledge of the so called "smearing matrix". In the Bayesian language this is given by the likelihood $P(E_j|C_i)$ that effect E_j is due to cause C_i. If $n_c(i)$ is the number of events generated in the bin i (cause C_i) and $n_e(j)$ is the measured number of events in the bin j (after all cuts), when $n_c(i)$ and $n_e(j)$ are sufficiently large, the probability $P(E_j|C_i)$ can be

estimated by

$$P(E_j|C_i) = \frac{n_e(j)}{n_c(i)} \tag{15}$$

In the $P(E_j|C_i)$ all effects due to the resolution and acceptance of the detector are included. Known the $P(E_j|C_i)$, the unfolded number of events in the bin i is given by:

$$\hat{n}(C_i) = \frac{1}{\epsilon_i} \sum_j n(E_j) P(C_i|E_j) \tag{16}$$

where $\epsilon_i = \sum_{j=1}^{n_E} P(E_j|C_i)$ is the efficiency of detecting an event generated in the bin C_i. The element $P(E_j|C_i)$ are evaluated using the Monte Carlo simulation , and $P(C_i|E_j)$ are calculated by the Bayes' theorem.

Bayes' theorem requires the knowledge of initial probability $P_o(C_i)$ for each cause C_i. A reasonable evaluation of these probabilities is given by the status of the art of the Monte Carlo simulation of the process of interest. In practice they have been calculated by the number of generated events for each cause (i.e. each physical bin) over the total number of events (in the sum are included also the background's cells, see later).

$$P_o(C_i) = \frac{N(C_i)}{\sum_i N(C_i)} \tag{17}$$

Obviously the unfolding returns also the final probability distribution $P(C_i)$. The closer the initial distribution $P_o(C_i)$ is to the true distribution, the better the agreement is. This suggests proceeding iteratively. To avoid the problems connected, in the iterative procedure, with statistical fluctuations, a smoothing of the unfolded distribution has been applied between two consecutive iterations. In fact the $n(C)$ distribution can be seen as points of the surface given by the differential cross section times the luminosity. So, a good smoothing function is every parametrization of the differential cross section. In this analysis the CKMT [14] parametrization has been used.

4.4.1 Treatment of background

The background can be seen as another cause which contributes to the effect E. Thus, all that one has just to do is to add to the physical cells C_{n_c} an extra cell C_{n_c+1}, with initial probability $P_o(C_{n_c+1})$. The result of unfolding will provide then the number of events to be assigned to the background. In the unfolding procedure three sources of background are included: photoproduction, *e-gas* and *p-gas*.

A fourth "background" has been added for convenience, due to all the DIS events generated outside the phase space of interest in this analysis. This

gives the possibility to take into account the migrations not only among the bins, but also between the bins and the rest of the phase space.

4.5 Results of F_2 with only Type A uncertainties (the "statistical errors" of the HEP jargon).

The unfolding procedure returns, known the measured distribution of events $n(\underline{\mathrm{E}})$, the best estimate of the "true" distribution of events $n(\underline{\mathrm{C}})$. Thus, knowing the guessed true number of events $N_{evt} \equiv n(C_i)$ in a bin, it is possible to evaluate F_2 through the measurement of the cross section as described above. In the table 1 the results of the analysis are reported step by step: number of events before and after the unfolding, the measured differential cross section, and finally the values of $\tilde{F}_2$ and F_2.

The high number of events in the bins gives a Type A uncertainties[1] between 2% and 5%, with a luminosity of only 236 nb^{-1}.

It should be noticed that the effect of the migrations makes the resulting numbers, and then the values of F_2, unavoidably correlated. The correlation matrix is evaluated automatically by the unfolding program. For all bins the correlation coefficient[2] ρ with the second neighbours is less than 4% except for the bin at $Q^2 = 0.6$ GeV^2 where it is around 10% along $y =$ k direction. With the first neighbours ρ is less than 45%, along $y =$ k direction, while it is less than 40% along $Q^2 =$ k direction, except for the lowest y bins, where the correlation is of the order of 70%. In the table 2 the correlation matrix due to Type A uncertainties is reported. The bin numbering is shown in figure 11.

It is important to stress that the Type B uncertainty due to possible systematic errors introduces further correlation among the measurements. This effect will be discussed in the next section.

[1] According to the ISO/BIPM recommendation [2] Type A uncertainties are *"those which are evaluated by statistical methods"*, in other words which depends on the collected "statistics". Type B uncertainties are instead *"those which are evaluated by other means"*. One has to notice that both kind of uncertainties have probabilistic meaning, thanks to the Bayesian approach, on which the cited recommendation is based.

[2] I remind that the correlation coefficient between the bin i and the bin j is defined by

$$\rho_{ij} = \frac{Cov(i,j)}{\sigma_i \sigma_j} \ . \tag{18}$$

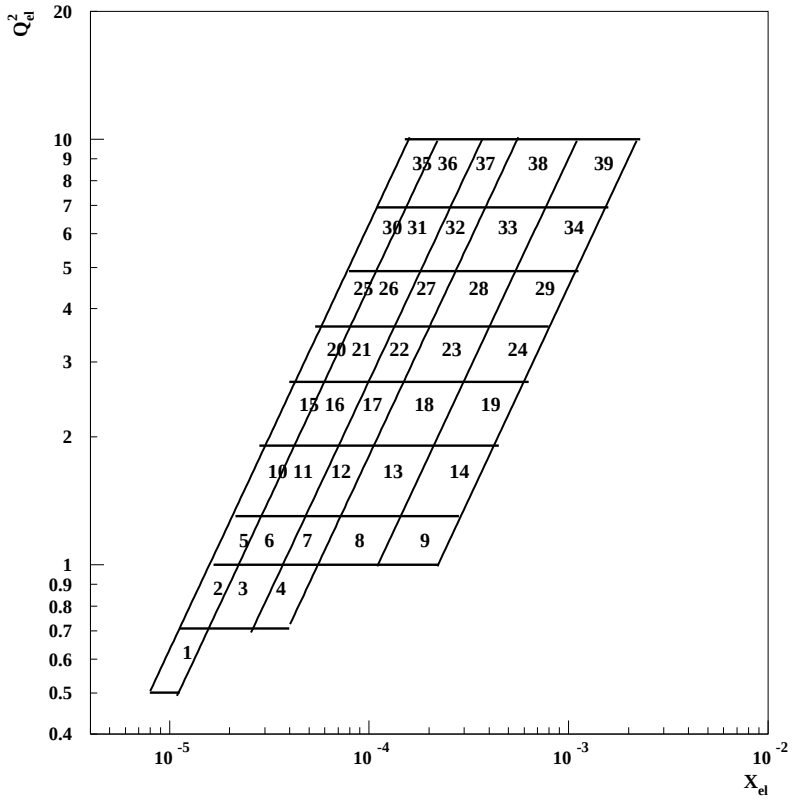

Figure 11: *The associated numbers to the bins used for the unfolding procedure and to evaluate the correlation matrix.*

5 Evaluation of Type B uncertainties (the "systematic errors").

The method used in this analysis to evaluate the uncertainties due to the systematic effects is first described. A derivation can be found in [15] and the practical formulae are the same as those given in [2].

Let us consider a certain number of $\underline{h}$ systematic "hypotheses" (all physics, Monte Carlo and detector parameters, as well as the analysis ones) and μ_{R_i} the value obtained when $\underline{h} = \underline{h}_o$. The corrected μ_i can be expressed as a function of μ_{R_i} and of a shift g_i due to the systematic effects $\underline{h}$.

$$\mu_i = \mu_{R_i} + g_i(\underline{h}) \tag{19}$$

Using Taylor's expansion we obtain, at first order,

$$\mu_i = \mu_{R_i} + \sum_l \frac{\partial g_i}{\partial h_l}(h_l - h_{ol}) \; . \tag{20}$$

(all derivatives are evaluated at $\underline{h} = \underline{h}_o$). Sometimes the expansion (20) is not performed around the best value of $\underline{h}$ but around their nominal values (for example a mass production of Monte Carlo events could have been generated with a parameter which does not reflect the present best knowledge on it), in the sense that the correction for the known value of systematic errors has not yet been applied. In this case, the best value of μ_i is then:

$$\hat{\mu}_i = E[\mu_i] \sim \mu_{R_i} + E[\sum_l \frac{\partial g_i}{\partial h_l}(h_l - h_{ol})] \equiv \mu_{R_i} + \sum_l \delta\mu_{il} \tag{21}$$

$$\sigma_i^2 = \sigma_{R_i}^2 + \sum_l \left(\frac{\partial g_i}{\partial h_l}\right)^2 \sigma_{h_l}^2 \equiv \sigma_{R_i}^2 + \sum_l u_{i_l}^2 \tag{22}$$

$$Cov(\mu_i, \mu_j) \sim \sum_l \left(\frac{\partial g_i}{\partial h_l}\right)\left(\frac{\partial g_j}{\partial h_l}\right) \sigma_{h_l}^2 \equiv \sum_l s_{ijl} u_{i_l} u_{j_l} \equiv \sum_l Cov_l(\mu_i, \mu_j) \tag{23}$$

where the correlations between the systematic hypotheses are assumed to be equal to zero (i.e. they are chosen to be as most independent as possible).

u_{i_l} can be seen as a component to the standard uncertainty due to the hypothesis h_l and s_{ijl} is the product of the sign of the derivatives. The shifts $\delta\mu_{il}$ are negligible if $g_i(h_l)$ is sufficient linear around h_{ol}.

$\frac{\partial g_i}{\partial h_l}$, called sensibility coefficient, describes the change of $\hat{\mu}_i$ given by a variation of h_l. The combined variance σ_i^2 can therefore be viewed as a sum of terms, the square roots of each, u_{i_l}, represents the standard uncertainty of the quantity caused on the uncertainty on the systematic effect h_l. It should be noticed that this probabilistic treatment of "systematic errors" is meaningful only if the probability is defined by "degree of belief" (the Bayesian definition) [2]. σ_{h_l} are then the standard deviation of the distribution which models our state of uncertainty about the h_l systematic effect.

For example, if one knows with almost certainty the range in which a quantity lies (let be x_1 and x_2 the limits of the intervals), but with no further knowledge about the values which are more or less reasonable, then a uniform distribution can be assumed (see figure 12). In many cases, on the other hand, a distribution that express well our uncertainty is the gaussian. Other useful distributions, also of interest for this analysis, are the triangular ones (see figure 12). The uncertainty associated to each systematic effect is measured by the standard deviation of the deviation of the distribution that models at best each case (see figure 12), as also recommended by ISO and

BIPM, rather than by probability intervals. In fact formulae (22)(23) apply to variances and covariance. It must be noticed that, although the sources of systematics effects may have different distributions, when "many"[3] uncertainties are combined together then the overall uncertainty can be described by a normal distribution, thanks to the Central Limit Theorem. It means that the results of this analysis, expressed by "best estimates $\pm\sigma$" have the usual meaning of 68% probability interval. When a component to the uncertainty is modeled by an asymmetric distribution the best estimate is shifted (as expressed by (21)) with respect to the value evaluated before the systematic effects (see the case of the asymmetric triangular distribution in figure 12).

In order to estimate u_{il} and $\delta\mu_{il}$ which enter in (22)(23) each hypotheses h_l was changed one at a time (either in the analysis procedure or at Monte Carlo level, depending on the source of systematics). Calling Δ_{h_l} the variation of h_l, then the corresponding variation of μ_i is given by

$$\Delta_{\mu_i} = \frac{\partial g_i}{\partial h_l}\Delta_{h_l} \tag{24}$$

It is easy to verify that when Δ_{h_l} are standard deviation, then (24) provides a practical way to get the terms needed in (22)(23). In particular, the practical formulae used for $\delta\mu_i$ and u_{il} are:

$$\begin{aligned} \delta\mu_{il} &= \frac{\mu_i(h_1,\cdots,h_l+\sigma_{h_l},\cdots,h_N)+\mu_i(h_1,\cdots,h_l-\sigma_{h_l},\cdots,h_N)}{2} - \mu_{R_i} \\ u_{il} &= \left|\frac{\mu_i(h_1,\cdots,h_l+\sigma_{h_l},\cdots,h_N)-\mu_i(h_1,\cdots,h_l-\sigma_{h_l},\cdots,h_N)}{2}\right| \end{aligned} \tag{25}$$

It should be noticed that this way to evaluate $\delta\mu_i$ takes into account implicitly of possible small non linearity of g_i, not considered in (21)(22)[4].

5.1 Sources of Type B uncertainties

According to the scheme described above, different analysis were carried out to estimate the systematic effects on F_2 measurement. Figure 13 shows the changes (in percentage) for each systematic hypotheses, due to a change of ± 1 standard deviation. This means that each systematic source is represented by two dots, corresponding to a change of +1 and -1 standard deviation.

[3]Many is in quotation marks because it is well known the fast convergence of the Central Limit Theorem for practical cases.

[4]To be even more precise one should consider the transformation of the distribution due to the non linear effects.

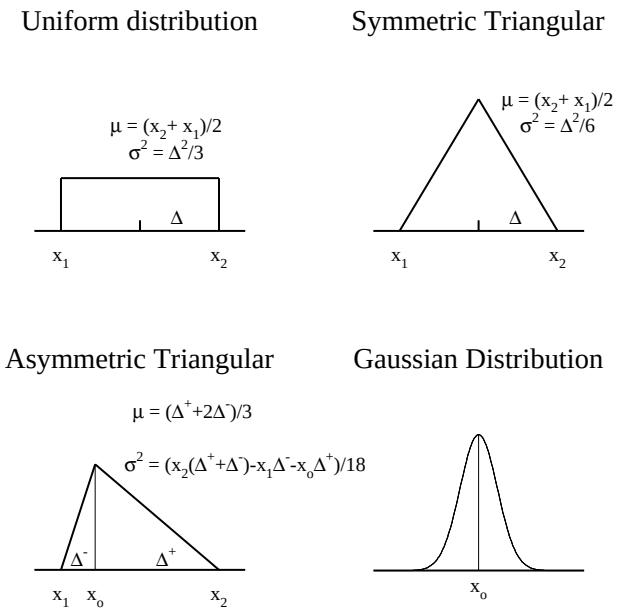

Figure 12: *Typical assumption on the systematic effects used to determine the Type B uncertainties: a) Uniform distribution b) Symmetric triangular distribution c) Asymmetric triangular distribution d) Gaussian distribution.*

Energy measurement

(1,2) As shown in figure 1, a shift less than 3% was observed in the measured energy for the KP events. A uniform distribution between 0 and 3% was assumed (0 means that no correction is applied to the measured energy). The parameters of the distribution are $E[h_1] = 1.5\%$ and $\sigma_{h_1} = 1\%$; this means that the energy in average was corrected by 1.5%. The contribution to the uncertainty of F_2 is of the order of 2.4% and, anyhow, less than 5% in all bins (see table 3).

(3,4) The higher value of +5% was found for an energy miscalibration in the calorimeter. Looking at the $(p_t^{el} - p_t^{had})$ distribution the higher shift registered is of the order of +8%. Assuming this value as upper value, the hadronic energy scale has been modeled by a triangular distribution with a standard deviation $\sigma_{h_2} = 3\%$. This gives a contribution to F_2 of the order of 1.3% and, in particular, less than 1% for $x < 10^{-4}$ and less 5% for $x > 10^{-4}$.

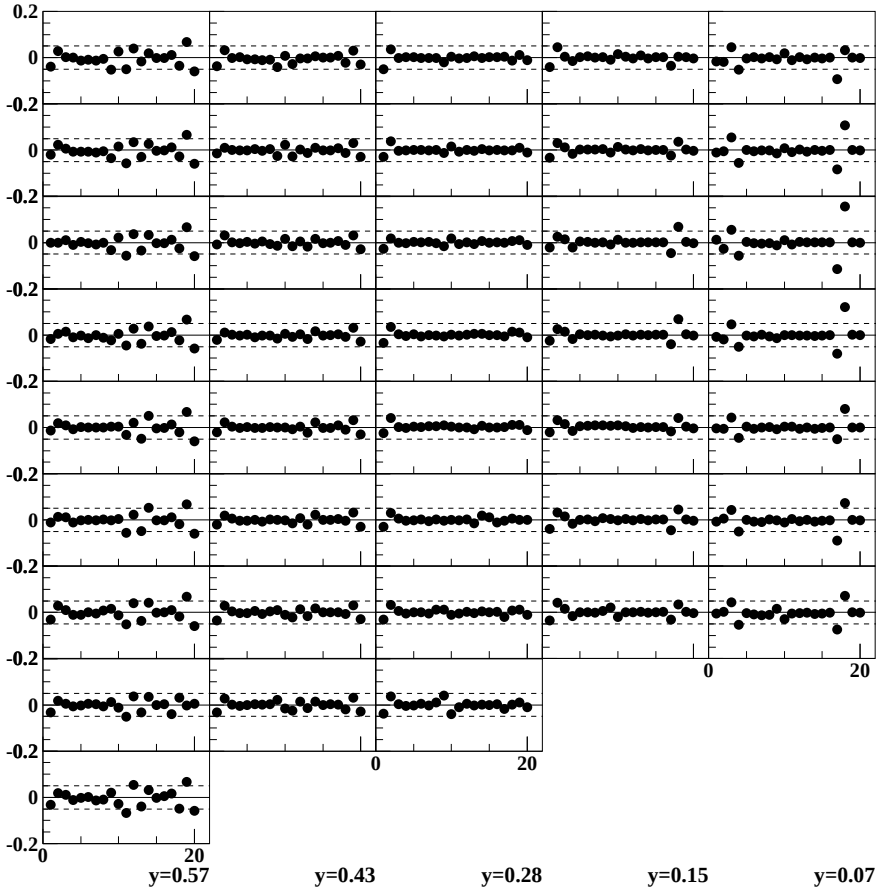

Figure 13: *For each bin the deviation in percentage are reported for each systematic source. The two dotted line in each plot indicate a* $\pm 5\%$ *contribution.*

Positron angle measurement

(5-8) The SRTD position was checked repeating the analysis for the X and Y axis separately. A gaussian distribution centered around the nominal value (i.e. 0 because the correction for the shift was just applied) with $\sigma_{h_3} = \sigma_{h_4} = 1$ mm was assumed for both axis. The bigger effects are less than 1% and, in average the contribution to F_2 is of the order of 0.3%.

(9,10) The vertex distribution is well reproduced by Monte Carlo except for the vertex given by satellite bunch. The uncertainty for the vertex measurement was checked changing the z vertex coordinate of $\sigma_{h_5} = 1.5$

cm, assuming a gaussian. This gives an uncertainty to F_2 of the order of 1.3%, with a change less than 3% in all bins.

Backgrounds

(11,12) In order to see the contribution given by the photoproduction events, it was assumed that the "true" number of events due to the photoproduction lays in a region between double and half of the measured events. Assuming an asymmetric triangular distribution in this region, centered around the measured number of events (i.e. looking the figure 12 x_o is the measured number of events, x_1 and x_2 are the half and the double of x_o), this distribution is characterized by a standard deviation $\sigma_{h_6} = 0.47$. The bigger effect on F_2 is less than 5% in the high y bins to become negligible in the low y region. On average the effect is around 1.7%.

(13,14) The same procedure used for the photoproduction events was applied to the *e-gas* and *p-gas* backgrounds. This gives a contribution less than 0.1% in all range of x and Q^2.

Kinematical cuts

(15,16) For the systematic effect due to the $E - P_z$ cut, a gaussian distribution with standard deviation $\sigma_{h_8} = 3$ GeV was assumed as model to describe our uncertainty on this cut. This gives a contribution to F_2 of 5% in the low x bin, becoming less than 2% at high x. In general the contribution is of the order of 1.1%.

(17,18) For the systematic check on the y_{JB} cut, a gaussian distribution with standard deviation $\sigma_{h_9} = 0.01$ was assumed as model.

Contribution is less 2% in the high y bin, while it is of 10-15% in low y bins, and on average it is 3.1%.

F_L contribution

(19,20) To check the contribution due to F_L the following procedure has been used. In principle F_L changes between 0 and F_2. Assuming the QCD as the best model, an asymmetric triangular distribution centered around its prediction (ZEUS NLO 94) and with lower and upper values between 0 ed F_2 has been taken. The standard deviation can be expressed in terms of F_2 and F_L: $\sigma_{h_{10}} = \sqrt{\frac{F_2^2 + F_L^2 - F_2 * F_L}{18}}$. The contributions on F_2 are of the order of 3.1% over the all phase space, but in

particular it is of the order of 6% in the high y bins and negligible in the low y region.

5.1.1 Additional Checks

In addition to the above systematic studies, other checks have been done to evaluate the consistence of the all procedure. These checks are not included in the evaluation of the total uncertainty.

- Using the new energy correction function, a new analysis has been done. This gives a contribution less than 1% in low y bins and less than 2% in the high y bins.

- The number of events without a tracks is not properly simulated. Probably most of these events come from the satellite bunch. So a new analysis was done putting the vertex at $z = 136$ cm, when no track is found. Contribution is less than 1% in all bins with $Q^2 < 6$ GeV^2 and between 3% and 7% in the high Q^2 bins (the bigger effect is in the low y region).

To summarize the uncertainty given by the systematic effects are between 4% and 15%. The bigger effects are shown in the high and low y bins, independently from Q^2. In the high y region the uncertainty is dominated by the inadequate dead material simulation and F_L contribution; at low y this is due to the noise and to the *electron method*. In addition there is a 2% error on the luminosity and trigger uncertainty. This uncertainty introduces another correlation among the measurements. In table 3, for each bin, the uncertainty given by each systematic hypotheses is shown, and in the table 4 the correlation matrix with the systematics' contribution is reported. Because a specific care is needed in treating normalization uncertainties, as discussed in [16], the effects of trigger efficiency and luminosity uncertainty are not included in the correlation matrix. Including these systematics, the covariant matrix of data will contain a sizable, overall uncertainty on the absolute normalization, and the use of this matrix in least square fits would produce biased results [16] (see also [17] and [18] for recent discussions on this problem).

6 Results

The results on the structure function F_2 vs x are shown in figure 14 at different Q^2. The F_2 values are corrected for the systematic shift according to (21) and the "statistical" and "systematic" uncertainty are reported according to (22). The uncertainty of luminosity and trigger efficiency (2%) is not shown.

Results (dots) are compared to '94 shifted SVX94 (triangle) and nominal (square) vertex data [1] and '95 preliminary BPC (diamond) results. There is in general a good agreement with '94 data, excepted in the high y bins, where SVX94 are higher. The rise of F_2 persists down to $Q^2 = 0.85$ GeV^2, but it is reduced strongly with decreasing Q^2.

In figure 15 the results are compared to some of the available parametrization based on pQCD like GRV [19] (dashed) and on Regge model like CKMT [14] (dotted line), ALLM [20] (dashed dotted). The ZEUS NLO fit '94 data, included the '94 shifted vertex data, is also shown (solid line). The ZEUS NLO 94 describes very well the data until to $Q^2 = 2.3$ GeV^2.

6.1 Total cross section $\sigma_{\gamma^* p}$

The DIS cross section can be viewed as the product of the flux of virtual photon times total cross section of photon proton scattering. So it is possible to write $\sigma_{\gamma^* p}$ in terms of longitudinal and transversal polarized photons.

$$\sigma_{\gamma^* p} \equiv \sigma_T + \sigma_L \tag{26}$$

Because F_2, in terms of σ_L e σ_T, is

$$F_2 = \frac{Q^2(1-x)}{4\pi^2\alpha}\frac{Q^2}{4m_p^2x^2 + Q^2}(\sigma_T + \sigma_L) \tag{27}$$

in the low x region, the $\sigma_{\gamma^* p}$ assumes the following expression:

$$\sigma_{\gamma^* p}(W^2, Q^2) \simeq \frac{4\pi^2\alpha}{Q^2}F_2(x, Q^2) \tag{28}$$

where $W^2 = m_p^2 + Q^2(\frac{1}{x} - 1)$ and m_p proton mass. Figure 16 shows $\sigma_{\gamma^* p}$ values at different $W^2 \sim \frac{Q^2}{x}$ for different Q^2. A smooth transition in Q^2 seems to emerge from this analysis.

6.2 Byproduct: a measurement of the average photoproduction total cross section

The unfolding method used allows, besides the main goal of this analysis, an interesting physical byproduct. In fact, the procedures allows to infer the

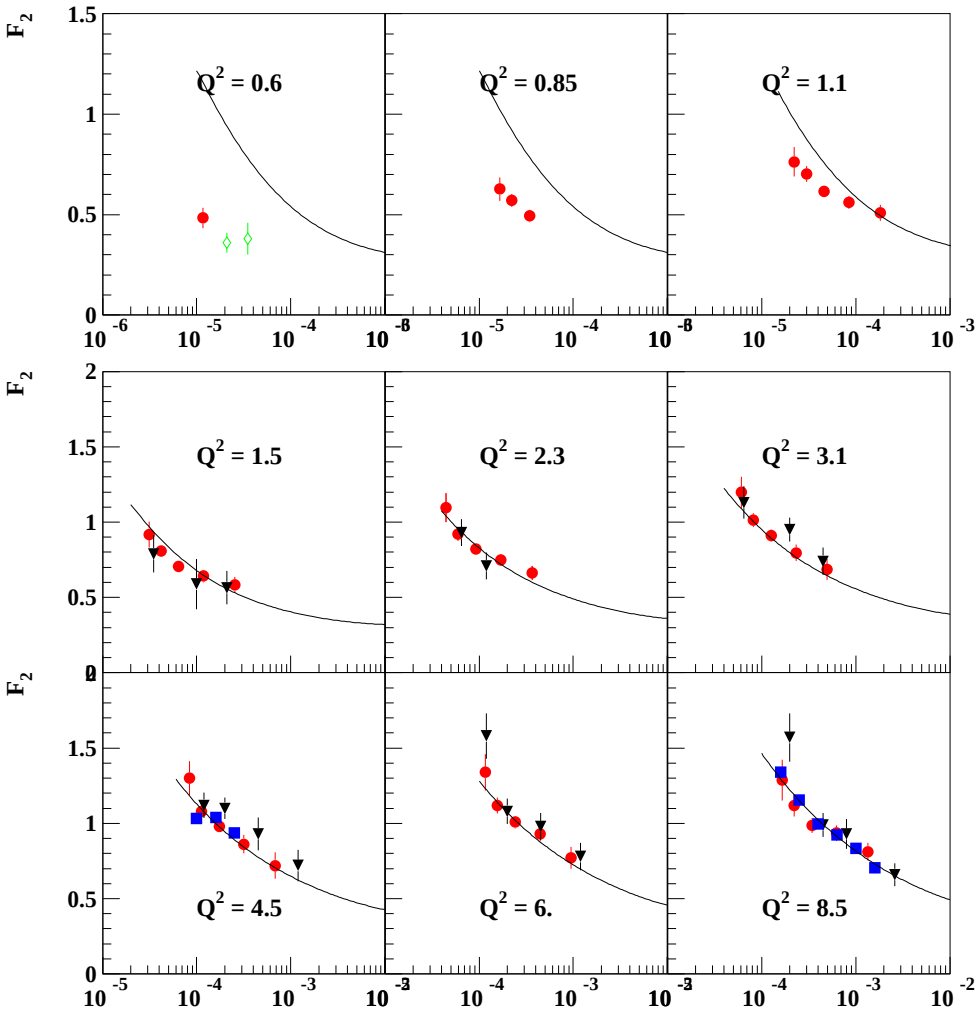

Figure 14: *Results on F_2 vs x compare with SVX94 (triangle), NVX94 (square), BPC (diamond) and ZEUS fit to all '94 data (solid line).*

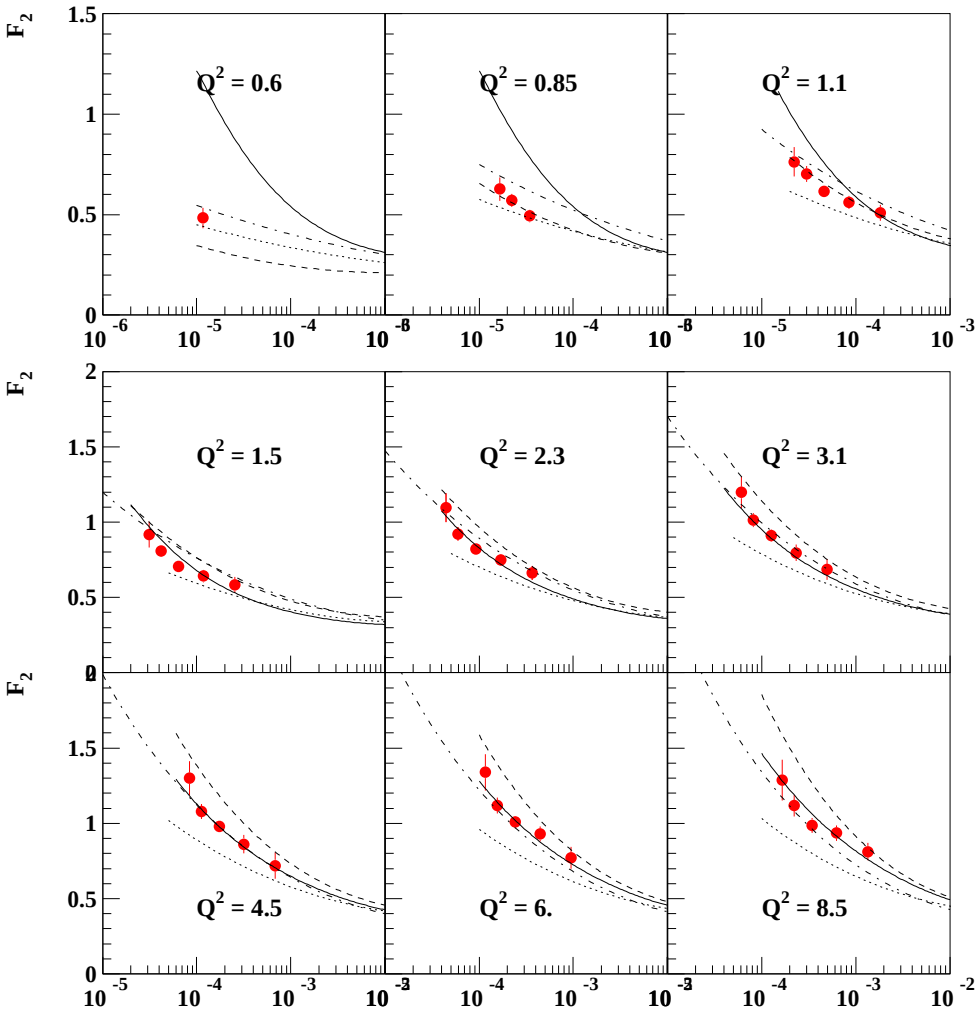

Figure 15: *Results on F_2 vs x compare with ZEUS fit to all '94 data (solid line), GRV (dashed line), CKMT (dotted line), ALLM (dotted and dashed line).*

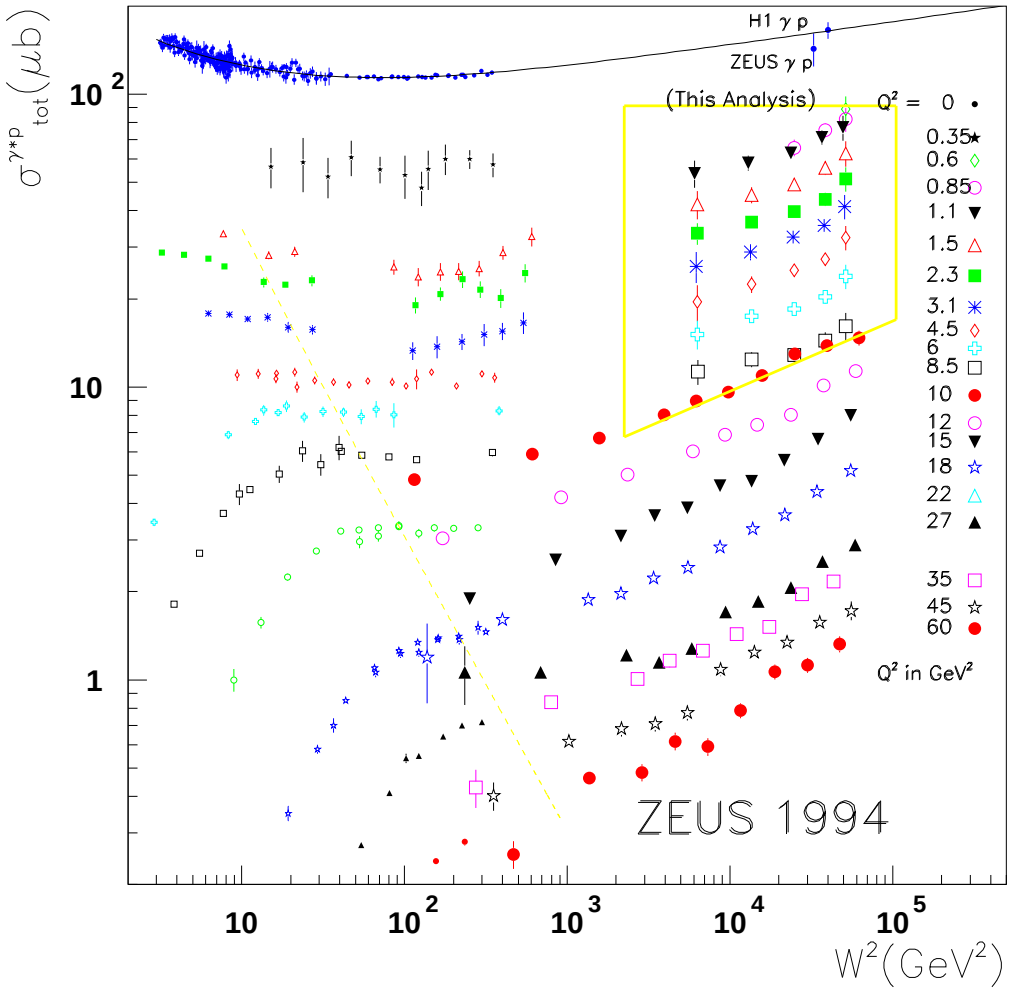

Figure 16: *Total cross section $\sigma_{\gamma^* p}$ vs W^2 at different Q^2.*

number of events associated to all the *causes* which can produce the observed data. The consistent treatment of the background according to this scheme, as described above, produces at the end of the unfolding the number of events to be attributed to a certain background. Considering the photoproduction background (PHP) the unfolding yields:

$$N(C_{PHP}) = (109 \pm 1) \cdot 10^3 \tag{29}$$

which becomes

$$N(C_{PHP}) = (111 \pm 8) \cdot 10^3 \tag{30}$$

when all the sources of systematics are considered, including that which varies by a large factor the "a priori" number of the photoproduction events (h_6). This number allows a measurement of the total photoproduction cross section. The PHP background, used in the unfolding, has been simulated in the range of $Q^2 < 2$ GeV^2. Assuming a constant cross section in Q^2, taking into account the efficiency of the selection cuts for the PHP events (ratio of PHP events that pass the cuts over all PHP events generated), the total cross section for photoproduction given by the unfolding is:

$$\sigma_{\gamma^* p}(Q^2 < 2\text{GeV}^2) = 99 \pm 8 \ \mu\text{b} \tag{31}$$

with a luminosity of $L = 236$ nb^{-1} and the efficiency $\epsilon = 0.00475$ (given by the ratio of the number of PHP events that pass the cuts over all the generated PHP events). In the low Q^2 region, x is $\sim 5 \cdot 10^{-5}$ on average; this means that for $Q^2 \sim 2$ GeV^2 we have $W^2 \sim 4 \cdot 10^4$. This can be compared with our expectation.

Taking at $Q^2 = 0$ GeV^2 and $W^2 \sim 4 \cdot 10^4$ then $\sigma_{\gamma p} = 156 \pm 20$ μb [21] and, for $Q^2 \sim 2$ GeV^2, $\sigma_{\gamma p} = 44 \pm 2$ μb. Thus, the average value is

$$E[\sigma_{\gamma^* p}(Q^2 < 2\text{GeV}^2)] = 100 \pm 20 \ \mu\text{b} \ , \tag{32}$$

in a "even too good" agreement. This analysis can, in principle, improve the knowledge of this quantity. However, one has to notice that the experimental result (31) has to be taken with some care. For example, it depends critically on the shape of the background assumed and a more refined study should be performed. In fact although this shape is not crucial for the F_2 analysis, it can be more critical for a result on the photoproduction itself.

7 Acknowlegments

I want to thank prof. Giulio D'Agostini that introduced me (with a Bayesian approach) in the ZEUS "world" and Dr. Elisabetta Gallo who helped me

in this "world". I'd also like to thank Rik Yoshida, J. T. Wu, Ludger Lindeman, Marcel Vreeswijk, Arnulf Quadt and prof. Egidio Longo for useful comments and routines. Moreover I'd like to thank the so called *Bolognesi*, *Padovani*, *Romani*, *Torinesi*, Dr. Vanna Pugliese, Dr. Giuseppe Barbagli and, in particular, Dr. Enrico Tassi.

References

[1] ZEUS Collaboration: M. Derrick et al. *DESY 96-076.*

[2] International Organization for Standardization (ISO) *Guide to the expression of uncertainty*, Geneva, 1993.

[3] G. A. Schuler and H. Spiesberger in *Proc. of the workshop on Physics at HERA.* vol. 3, p. 1409.

[4] H-J. Mohring et al. *DESY 90-041.*

[5] G. Ingelman et al. *Proc. "Physics at HERA"*, ed. W. Buchmueller, vol. 3 1366 DESY 1992.

[6] L. Lonnblad *Comput. Phys. Commun.* 71, 1992.

[7] A. D. Martin,R. G. Roberts e W. J. Stirling *Phys. Rev.* **D51** (1995) 425.

[8] E. Gallo ZEUS-Note 96-001 *The TLT and DST filters for the DIS group in 1995*

[9] J. NG e W. Verkerke. *An Overview of SRTD Analysis.* ZEUS-Note 95-037.

[10] Trasparency presented by Ludger Lindemann at (old) DIS friday meeting.

[11] H.-U. Bengtsson e T. Sjostrand *PYTHIA 5.6 Comput. Phys. Commun.*, 46, 1987.

[12] Routine zeus46.f of Marcel Vreeswijk which includes also the 94 shifted vertex data and it is avaible in the zow cluster in marcel/zeus46.f .

[13] G. D'Agostini *Nucl. Instr. Meth.* **A362** (1995) 487.

[14] A. Capella et al. *Phys. Lett.* **B 337:358**, 1994.

[15] G. D'Agostini *Probability and Measurement Uncertainity in Physics - a Bayesian Primer*- DESY 95-242

[16] G. D'Agostini, *Nucl. Instr. and Meth. in Phys. Res.* **A346** (1994) 306.

[17] Tatsu Takeuchi *The status of the Determination of* $\alpha(m_Z)$ *and* $\alpha_s(m_Z)$, hep-ph/9603415.

[18] S. Alekhin *Extraction of parton distribution and* α_s *from DIS data within the Bayesian treatment of systematic errors*, hep-ph/9611213.

[19] M. Gluck, E. Reya e A. Vogt *Z. Phys.* **C67**, 443 (1995).

[20] H. Abramowicz, E. M. Levin, A. Levy e U. Maor *Phys. Lett.* **B269** (1991) 465.

[21] G. Wolf *HERA Physics* , DESY 94-022.

[22] H1 Collaboration *A Mesaurement of the Proton Structure Function* F_2 *at low x and low* Q^2 *at HERA* Warsaw pre-print.

Q^2 (GeV^2)	y	x	$N_{obs.}$	$N_{unf} \pm \delta N$	$\frac{d^2\sigma}{dydQ^2} \pm \delta\sigma$ (10^2nb/GeV^2)	$\tilde{F}_2 \pm \delta\tilde{F}_2$	$F_2 \pm \delta F_2$
0.6	0.57	$1.16{\cdot}10^{-5}$	472	2472 ± 63	3.67 ± 0.11	0.488±0.014	0.488±0.014
0.85	0.57	$1.65{\cdot}10^{-5}$	808	2317 ± 46	2.29 ± 0.06	0.614± 0.015	0.635±0.015
	0.43	$2.21{\cdot}10^{-5}$	1196	3496 ± 63	3.20 ± 0.07	0.567± 0.012	0.576± 0.010
	0.28	$3.42{\cdot}10^{-5}$	1075	5527 ± 104	4.94 ± 0.11	0.495 ± 0.010	0.497± 0.010
1.1	0.57	$2.23{\cdot}10^{-5}$	641	1501 ± 30	1.50 ± 0.04	0.734± 0.021	0.763± 0.022
	0.43	$2.99{\cdot}10^{-5}$	1150	2310 ± 38	2.14 ± 0.04	0.695±0.014	0.708±0.014
	0.28	$4.63{\cdot}10^{-5}$	1603	3666 ± 57	3.35 ± 0.06	0.613±0.014	0.617±0.014
	0.15	$8.49{\cdot}10^{-5}$	1434	4721 ± 72	6.32 ± 0.11	0.560±0.010	0.559±0.010
	0.07	$1.82{\cdot}10^{-4}$	872	6604 ± 127	13.5 ± 0.4	0.516±0.013	0.516± 0.013
1.5	0.57	$3.11{\cdot}10^{-5}$	1222	1860 ± 35	0.92 ± 0.02	0.872±0.019	0.916±0.019
	0.43	$4.17{\cdot}10^{-5}$	1695	2750 ± 41	1.26 ± 0.02	0.793±0.015	0.812±0.015
	0.28	$6.44{\cdot}10^{-5}$	2347	4382 ± 61	1.99 ± 0.03	0.705± 0.013	0.711± 0.013
	0.15	$1.18{\cdot}10^{-4}$	2454	5644 ± 74	3.77 ± 0.07	0.646±0.010	0.648± 0.010
	0.07	$2.53{\cdot}10^{-4}$	1833	7788 ± 121	7.94 ± 0.18	0.586±0.010	0.586± 0.010
2.3	0.57	$4.47{\cdot}10^{-5}$	1111	1397 ± 26	0.52 ± 0.013	1.02±0.024	1.08±0.026
	0.43	$5.99{\cdot}10^{-5}$	1745	1991 ± 31	0.69 ± 0.014	0.894±0.015	0.919±0.016
	0.28	$9.26{\cdot}10^{-5}$	2382	3184 ± 44	1.09 ± 0.02	0.798±0.011	0.806±0.011
	0.15	$1.69{\cdot}10^{-4}$	2186	4073 ± 54	2.05 ± 0.05	0.727±0.010	0.729±0.010
	0.07	$3.64{\cdot}10^{-4}$	1597	5547 ± 87	4.26 ± 0.09	0.650±0.012	0.650±0.012
3.1	0.57	$6.12{\cdot}10^{-5}$	804	934 ± 21	0.31 ± 0.009	1.14±0.032	1.22±0.034
	0.43	$8.21{\cdot}10^{-5}$	1330	1316 ± 23	0.41 ± 0.009	0.993±0.018	1.02±0.019
	0.28	$1.27{\cdot}10^{-4}$	2041	2145 ± 33	0.66 ± 0.013	0.904±0.013	0.914±0.013
	0.15	$2.33{\cdot}10^{-4}$	2011	2637 ± 37	1.19 ± 0.022	0.792±0.015	0.794±0.015
	0.07	$4.98{\cdot}10^{-4}$	1319	3480 ± 58	2.39 ± 0.06	0.685±0.018	0.686±0.018
4.5	0.57	$8.35{\cdot}10^{-5}$	721	836± 21	0.18 ± 0.006	1.22±0.036	1.30± 0.038
	0.43	$1.12{\cdot}10^{-4}$	1207	1145± 22	0.23 ± 0.004	1.03±0.020	1.06± 0.020
	0.28	$1.73{\cdot}10^{-4}$	2002	1923± 30	0.38 ± 0.004	0.967±0.015	0.978±0.015
	0.15	$3.17{\cdot}10^{-4}$	2218	2380 ± 34	0.69 ± 0.007	0.853±0.012	0.856±0.012
	0.07	$6.80{\cdot}10^{-4}$	1417	3008 ± 52	1.31 ± 0.02	0.700±0.013	0.700±0.013
6.	0.57	$1.16{\cdot}10^{-4}$	482	635 ± 20	0.096 ± 0.0004	1.27±0.044	1.36±0.047
	0.43	$1.56{\cdot}10^{-4}$	945	879 ± 20	0.12 ± 0.004	1.08±0.023	1.12±0.024
	0.28	$2.41{\cdot}10^{-4}$	1539	1447 ± 27	0.20 ± 0.005	0.992±0.016	1.003±0.016
	0.15	$4.43{\cdot}10^{-4}$	1792	1889 ± 30	0.38 ± 0.008	0.927±0.02	0.925±0.02
	0.07	$9.49{\cdot}10^{-4}$	1199	2433 ± 45	0.74 ± 0.02	0.763±0.016	0.764±0.016
8.5	0.57	$1.65{\cdot}10^{-4}$	176	460 ± 24	0.047 ± 0.003	1.244±0.06	1.327±0.07
	0.43	$2.21{\cdot}10^{-4}$	567	684 ± 20	0.064 ± 0.003	1.133±0.03	1.169±0.03
	0.28	$3.42{\cdot}10^{-4}$	1144	1097 ± 26	0.10 ± 0.003	1.00±0.031	1.013 ±0.031
	0.15	$6.28{\cdot}10^{-4}$	1339	1463 ± 30	0.20 ± 0.004	0.949±0.025	0.953±0.025
	0.07	$1.34{\cdot}10^{-3}$	1102	2019 ± 47	0.40 ± 0.005	0.832±0.02	0.832±0.02

Table 1: *In the table are reported the principal steps of the analysis, before the systematics' studies. δ N, $\delta\tilde{F}_2$ and δF_2 stay for the standard uncertainties.*

	1	2	3	4	5	6	7	8	9	10	11	12	13	14	15	16	17	18	19	20	21	22	23	24	25	26	27	28	29	30	31	32	33	34	35	36	37	38	39
1	1.	.48	.26	.06	.11	.08	.03	.01	0	.03	.03	.01	0	0	.04	.03	0	0	0	.02	.02	0	0	0	0	.02	0	0	0	0	0	0	0	0	0	0	0	0	0
2	.48	1.	.37	.07	.41	.31	.06	0	0	.09	.10	.03	0	0	.03	.02	0	0	0	.02	.01	0	-.01	0	.01	.01	0	-.01	0	0	.01	0	0	0	0	0	0	0	0
3	.26	.37	1.	.38	.13	.45	.22	.06	.01	.03	.10	.06	.02	0	.01	.02	.01	0	0	0	.01	0	0	0	0	.01	0	0	-.01	0	0	0	0	0	0	0	0	0	0
4	.06	.07	.38	1.	.03	.17	.46	.23	.05	.01	.05	.10	.04	.01	0	0	.02	.01	0	0	0	.01	0	0	0	0	0	0	0	0	0	0	0	0	0	0	0	0	0
5	.11	.41	.13	.03	1.	.32	.04	0	0	.43	.33	.05	0	0	.06	.06	.03	0	0	.02	.01	.01	0	0	.02	.01	0	0	0	.01	.01	0	0	0	0	0	0	0	0
6	.08	.31	.45	.17	.32	1.	.31	.06	.01	.10	.41	.23	.05	.01	.02	.05	.03	.01	0	0	.02	0	-.01	-.01	0	.01	0	-.01	-.01	0	0	0	0	-.01	0	0	0	-.01	0
7	.03	.06	.22	.46	.04	.31	1.	.42	.10	.01	.12	.39	.19	.05	0	.01	.04	.02	.01	0	0	.01	0	-.01	0	0	0	0	-.01	0	0	0	0	0	0	0	0	0	0
8	.01	0	.06	.23	0	.06	.42	1.	.67	0	.04	.17	.36	.27	0	0	.01	.05	.04	0	0	0	0	0	0	0	0	0	0	0	0	0	0	0	0	0	0	-.01	0
9	0	0	.01	.05	0	.01	.10	.67	1.	0	.01	.05	.24	.36	0	0	0	.03	.05	0	0	0	0	0	0	0	-.01	0	0	0	0	0	0	0	0	0	0	0	0
10	.03	.09	.03	.01	.43	.10	.01	0	0	1.	.35	.04	0	0	.33	.23	.06	0	0	.04	.04	.02	0	0	.02	0	0	0	0	0	0	0	-.01	0	0	0	0	0	0
11	.03	.10	.10	.05	.33	.41	.12	.04	.01	.35	1.	.35	.05	.01	.09	.28	.21	.06	.02	.02	.03	.02	0	0	0	0	0	-.01	-.01	0	.01	0	0	-.01	0	0	0	0	0
12	.01	.03	.06	.10	.05	.23	.39	.17	.05	.04	.35	1.	.38	.12	.02	.08	.24	.17	.07	0	0	.03	.01	.01	0	0	0	0	0	0	0	0	0	-.01	0	0	0	0	0
13	0	0	.02	.04	0	.05	.19	.36	.24	0	.05	.38	1.	.66	0	.02	.08	.24	.23	0	0	0	.02	.03	0	0	0	0	0	0	0	0	0	0	0	0	-.01	0	-.01
14	0	0	0	.01	0	.01	.05	.27	.36	0	.01	.12	.66	1.	0	.01	.03	.13	.26	0	0	0	.01	.03	0	0	0	0	.01	0	0	-.01	0	0	0	0	0	0	0
15	.04	.03	.01	0	.06	.02	0	0	0	.33	.09	.02	0	0	1.	.35	.04	0	0	.36	.25	.04	0	0	.05	.05	.02	0	0	.01	0	0	0	0	0	0	0	0	0
16	.03	.02	.02	0	.06	.05	.01	0	0	.23	.28	.08	.02	.01	.35	1.	.34	.06	.01	.08	.29	.19	.05	.01	.02	.04	.02	.01	0	0	.01	0	-.01	-.01	0	0	0	-.01	0
17	0	0	.01	.02	.03	.03	.04	.01	0	.06	.21	.24	.08	.03	.04	.34	1.	.42	.13	.01	.07	.24	.18	.07	0	.01	.02	0	0	0	0	0	0	-.01	0	0	0	0	0
18	0	0	0	.01	0	.01	.02	.05	.03	0	.06	.17	.24	.13	0	.06	.42	1.	.70	0	.02	.07	.22	.23	0	0	.01	.01	.02	0	0	0	0	0	0	0	0	0	0
19	0	0	0	0	0	0	.01	.04	.05	0	.02	.07	.23	.26	0	.01	.13	.70	1.	0	.01	.03	.11	.22	0	0	0	.01	.02	0	0	0	0	0	0	0	0	0	0
20	.02	.02	0	0	.02	0	0	0	0	.04	.02	0	0	0	.36	.08	.01	0	0	1.	.29	.03	0	0	.36	.24	.03	0	0	.05	.02	.01	0	0	.01	.01	0	0	0
21	.02	.01	.01	0	.01	.02	0	0	0	.04	.03	0	0	0	.25	.29	.07	.02	.01	.29	1.	.28	.04	.01	.06	.28	.18	.04	0	.01	.02	.01	0	0	0	.01	0	0	0
22	0	0	0	.01	.01	0	.01	0	0	.02	.02	.03	0	0	.04	.19	.24	.07	.03	.03	.28	1.	.37	.10	.01	.07	.25	.13	.04	0	.01	.02	.01	0	0	0	0	0	0
23	0	-.01	0	0	0	-.01	0	0	0	0	0	.01	.02	.01	0	.05	.18	.22	.11	0	.04	.37	1.	.65	0	.02	.07	.20	.19	0	0	.01	.01	.01	0	0	0	0	0
24	0	0	0	0	0	-.01	-.01	0	0	0	0	.01	.03	.03	0	.01	.07	.23	.22	0	.01	.10	.65	1.	0	0	.02	.10	.20	0	0	0	.01	.02	0	0	0	0	0
25	0	.01	0	0	.02	0	0	0	0	.02	0	0	0	0	.05	.02	0	0	0	.36	.06	.01	0	0	1.	.29	.03	0	0	.38	.20	.03	0	0	.06	.05	.01	0	0
26	.02	.01	.01	0	.01	.01	0	0	0	0	0	0	0	0	.05	.04	.01	0	0	.24	.28	.07	.02	0	.29	1.	.29	.04	0	.09	.26	.13	.02	0	.01	.03	.01	0	0
27	0	0	0	0	0	0	0	0	-.01	0	0	0	0	0	.02	.02	.02	.01	0	.03	.18	.25	.07	.02	.03	.29	1.	.35	.08	.01	.06	.20	.13	.04	0	.01	.01	0	0
28	0	-.01	0	0	0	-.01	0	0	0	0	-.01	0	0	0	0	.01	0	.01	.01	0	.04	.13	.20	.10	0	.04	.35	1.	.62	0	.01	.05	.17	.18	0	0	0	.01	.01
29	0	0	-.01	0	0	-.01	-.01	0	0	0	-.01	0	0	.01	0	0	0	.02	.02	0	0	.04	.19	.20	0	0	.08	.62	1.	0	0	.02	.07	.17	0	0	0	.01	.01
30	0	0	0	0	.01	0	0	0	0	0	0	0	0	0	.01	0	0	0	0	.05	.01	0	0	0	.38	.09	.01	0	0	1.	.31	.03	0	0	.34	.25	.03	0	0
31	0	.01	0	0	.01	0	0	0	0	0	0	.01	0	0	0	0	.01	0	0	0	.02	.02	.01	0	0	.20	.26	.06	.01	0	.31	1.	.26	.04	0	.06	.25	.14	.03	0
32	0	0	0	0	0	0	0	0	0	0	0	0	0	-.01	0	0	0	0	0	.01	.01	.02	.01	0	.03	.13	.20	.05	.02	.03	.26	1.	.39	.07	.01	.06	.20	.10	.03
33	0	0	0	0	0	0	0	0	0	-.01	0	0	0	0	0	-.01	0	0	0	0	0	.01	.01	.01	0	.02	.13	.17	.07	0	.04	.39	1.	.65	0	.01	.06	.17	.15
34	0	0	0	0	0	-.01	0	0	0	0	-.01	-.01	0	0	0	-.01	-.01	0	0	0	0	0	.01	.02	0	0	.04	.18	.17	0	0	.07	.65	1.	0	.01	.02	.08	.15
35	0	0	0	0	0	0	0	0	0	0	0	0	0	0	0	0	0	0	0	.01	0	0	0	0	.06	.01	0	0	0	.34	.06	.01	0	0	1.	.34	.04	.01	0
36	0	0	0	0	0	0	0	0	0	0	0	0	0	0	0	0	0	0	0	.01	.01	0	0	0	.05	.03	.01	0	0	.25	.25	.06	.01	.01	.34	1.	.35	.04	0
37	0	0	0	0	0	0	0	0	0	0	0	0	-.01	0	0	0	0	0	0	0	0	0	0	0	.01	.01	.01	0	0	.03	.14	.20	.06	.02	.04	.35	1.	.36	.08
38	0	0	0	0	0	-.01	0	-.01	0	0	0	0	0	0	0	-.01	0	0	0	0	0	0	0	0	0	0	0	.01	.01	0	.03	.10	.17	.08	.01	.04	.36	1.	.64
39	0	0	0	0	0	0	0	0	0	0	0	0	-.01	0	0	0	0	0	0	0	0	0	0	0	0	0	0	.01	.01	0	0	.03	.15	.15	0	0	.08	.64	1.

Table 2: *The correlation matrix between F_2 values, calculated before the systematic effects are taken into account, is shown. The bin corresponding to each row or column is shown in figure 11.*

Q^2 (GeV^2)	y	x	F_2	$u_t \cdot 10^{-2}$	$u_1 \cdot 10^{-2}$	$u_2 \cdot 10^{-2}$	$u_3 \cdot 10^{-2}$	$u_4 \cdot 10^{-2}$	$u_5 \cdot 10^{-2}$	$u_6 \cdot 10^{-2}$	$u_7 \cdot 10^{-2}$	$u_8 \cdot 10^{-2}$	$u_9 \cdot 10^{-2}$	$u_{10} \cdot 10^{-2}$
0.6	0.57	$1.16 \cdot 10^{-5}$	0.483	5.0	1.5	.09	0.2	0.2	1.2	2.	0.06	1.9	1.1	3.2
0.85	0.57	$1.65 \cdot 10^{-5}$	0.627	5.8	1.6	0.18	0.16	0.04	0.078	3.0	0.059	1.7	0.9	4.0
	0.43	$2.21 \cdot 10^{-5}$	0.571	3.3	1.7	0.09	0.08	0.11	1.1	1.2	0.02	0.8	0.3	1.7
	0.28	$3.42 \cdot 10^{-5}$	0.493	3.2	1.9	0.21	0.25	0.28	2.1	0.5	0.03	0.34	0.6	0.6
1.1	0.57	$2.23 \cdot 10^{-5}$	0.763	7.4	2.2	0.55	0.36	0.33	0.92	4.2	0.08	2.0	0.9	4.8
	0.43	$2.99 \cdot 10^{-5}$	0.702	3.9	2.2	0.21	0.28	0.27	0.71	1.7	0.03	0.7	0.1	2.1
	0.28	$4.63 \cdot 10^{-5}$	0.616	2.7	1.9	0.36	0.09	0.48	0.77	0.41	0.01	0.02	0.8	0.7
	0.15	$8.49 \cdot 10^{-5}$	0.561	3.4	2.1	1.03	0.02	0.2	1.2	0.05	0.05	0.19	1.9	0.2
	0.07	$1.81 \cdot 10^{-4}$	0.509	5.6	0.07	2.6	0.09	0.17	1.2	0.3	0.05	0.4	4.6	0.03
1.5	0.57	$3.11 \cdot 10^{-5}$	0.918	8.9	1.2	0.81	0.17	0.1	0.25	6.0	0.1	1.9	1.1	5.7
	0.43	$4.17 \cdot 10^{-5}$	0.809	4.1	1.6	0.3	0.0	0.23	0.1	2.4	0.04	0.5	0.4	2.4
	0.28	$6.44 \cdot 10^{-5}$	0.707	2.8	2.2	0.3	0.02	0.23	0.02	0.6	0.	0.09	0.8	0.8
	0.15	$1.18 \cdot 10^{-4}$	0.642	4.1	2.3	1.1	0.	0.4	0.3	0.	0.04	0.3	2.9	0.2
	0.07	$2.53 \cdot 10^{-4}$	0.582	6.6	0.3	2.8	0.1	0.3	0.4	0.4	0.02	0.1	5.8	0.04
2.3	0.57	$4.47 \cdot 10^{-5}$	1.096	10.0	1.8	0.6	0.2	0.1	0.09	6.4	0.1	2.	1.6	6.7
	0.43	$5.99 \cdot 10^{-5}$	0.922	4.6	2.	0.1	0.3	0.1	0.	2.6	0.04	0.1	0.8	2.7
	0.28	$9.26 \cdot 10^{-5}$	0.823	3.2	2.6	0.2	0.1	0.05	0.3	0.7	0.02	0.08	0.1	0.9
	0.15	$1.69 \cdot 10^{-4}$	0.748	3.4	2.	1.2	0.06	0.05	0.2	0.03	0.05	0.4	2.1	0.2
	0.07	$3.64 \cdot 10^{-4}$	0.663	5.9	0.03	2.7	0.1	0.1	0.1	0.5	0.	0.06	5.	0.04
3.1	0.57	$6.12 \cdot 10^{-5}$	1.197	10.9	1.3	0.9	0.7	0.9	1.7	5.3	0.08	4.1	1.9	7.6
	0.43	$8.21 \cdot 10^{-5}$	1.012	4.7	1.6	0.	0.5	0.1	0.9	2.1	0.02	0.5	0.9	3.
	0.28	$1.27 \cdot 10^{-4}$	0.911	3.7	3.1	0.3	0.4	0.08	3.	0.2	0.6	0.02	0.08	0.9
	0.15	$2.32 \cdot 10^{-4}$	0.796	5.1	2.	1.4	0.2	0.1	0.02	0.	0.06	0.2	4.3	0.2
	0.07	$4.98 \cdot 10^{-4}$	0.685	8.6	0.3	3.2	0.1	0.2	0.3	0.4	0.04	0.	7.7	0.09
4.5	0.57	$8.35 \cdot 10^{-5}$	1.30	11.9	0.02	0.7	0.3	0.5	3.4	4.4	0.06	5.4	2.2	8.1
	0.43	$1.12 \cdot 10^{-4}$	1.07	5.1	2.	0.	0.4	0.6	1.5	1.7	0.04	1.	1.	3.1
	0.28	$1.73 \cdot 10^{-4}$	0.978	3.3	2.2	0.1	0.02	0.2	1.4	0.6	0.05	0.3	0.1	1.
	0.15	$3.17 \cdot 10^{-4}$	0.862	5.6	2.2	1.6	0.1	0.08	0.06	0.	0.08	0.08	4.67	0.2
	0.07	$6.80 \cdot 10^{-4}$	0.719	10.6	1.2	3.7	0.2	0.05	0.7	0.2	0.07	0.2	9.7	0.04
6.	0.57	$1.17 \cdot 10^{-4}$	1.33	12.4	2.8	0.7	0.3	0.3	3.3	3.4	0.02	5.4	2.4	8.3
	0.43	$1.56 \cdot 10^{-4}$	1.118	5.5	1.1	0.02	0.5	0.3	2.5	1.2	0.03	1.4	1.1	3.2
	0.28	$2.42 \cdot 10^{-4}$	1.008	4.1	3.3	0.	0.1	0.1	1.1	0.3	0.09	0.3	0.3	1.1
	0.15	$4.43 \cdot 10^{-4}$	0.929	4.6	3.	1.4	0.1	0.2	0.9	0.2	0.1	0.2	2.6	0.3
	0.07	$9.49 \cdot 10^{-4}$	0.770	9.1	0.7	3.8	0.2	0.01	1.	0.3	0.1	0.	7.9	0.05
8.5	0.57	$1.65 \cdot 10^{-4}$	1.287	13.6	3.8	0.2	0.7	0.6	4.9	2.	0.07	4.9	2.6	8.
	0.43	$2.21 \cdot 10^{-4}$	1.118	7.2	3.9	0.08	0.2	0.2	2.6	0.5	0.09	1.4	1.7	3.4
	0.28	$3.42 \cdot 10^{-4}$	0.987	5.4	4.4	0.04	0.2	0.07	1.1	0.2	0.1	0.01	0.95	1.1
	0.15	$6.28 \cdot 10^{-4}$	0.936	5.5	4.4	1.3	0.08	0.2	1.	0.4	0.1	0.4	1.8	0.3
	0.07	$1.34 \cdot 10^{-3}$	0.812	8.3	0.9	3.6	0.03	0.02	1.6	0.3	0.2	0.09	6.7	0.05

Table 3: *For each bin, the corrected (for the systematic effects) value of F_2, the total uncertainty and the contribution for each systematic, are presented. The uncertainty due to trigger efficiency and luminosity is not shown (see text).*

	1	2	3	4	5	6	7	8	9	10	11	12	13	14	15	16	17	18	19	20	21	22	23	24	25	26	27	28	29	30	31	32	33	34	35	36	37	38	39
1	1.	.94	.89	.53	.92	.85	.46	.16	-.11	.84	.83	.44	.04	-.18	.86	.80	.53	.05	-.23	.82	.74	.44	-.06	-.24	.73	.69	.40	-.07	-.26	.76	.58	.42	.03	-.21	.62	.54	.35	.10	-.21
2	.94	1.	.87	.45	.96	.87	.45	.15	-.08	.92	.89	.48	.07	-.13	.93	.86	.55	.09	-.16	.88	.81	.47	0	-.16	.78	.76	.47	0	-.17	.79	.63	.44	.08	-.13	.65	.56	.34	.12	-.12
3	.89	.87	1.	.74	.86	.93	.68	.42	.02	.73	.82	.63	.28	-.04	.76	.79	.71	.29	-.11	.67	.67	.62	.15	-.12	.54	.63	.47	.12	-.16	.63	.45	.52	.24	-.08	.51	.52	.47	.31	-.08
4	.53	.45	.74	1.	.48	.67	.83	.76	.35	.28	.46	.64	.56	.26	.30	.41	.65	.53	.16	.16	.21	.57	.41	.15	.00	.16	.22	.35	.08	.13	-.04	.35	.39	.16	.06	.16	.35	.42	.11
5	.92	.96	.86	.48	1.	.89	.50	.20	-.04	.94	.93	.52	.13	-.08	.94	.88	.58	.15	-.12	.87	.81	.50	.05	-.12	.77	.75	.48	.05	-.13	.78	.63	.45	.14	-.08	.64	.55	.35	.17	-.07
6	.85	.87	.93	.67	.89	1.	.73	.44	.04	.78	.90	.73	.35	.01	.80	.84	.76	.36	-.05	.71	.74	.69	.22	-.06	.58	.69	.58	.21	-.10	.67	.53	.61	.35	.00	.57	.59	.53	.41	.01
7	.46	.45	.68	.83	.50	.73	1.	.84	.39	.34	.56	.87	.75	.38	.35	.52	.79	.72	.31	.23	.37	.77	.60	.28	.10	.34	.50	.57	.22	.25	.15	.57	.66	.35	.22	.36	.55	.68	.33
8	.16	.15	.42	.76	.20	.44	.84	1.	.73	.05	.25	.74	.91	.69	.05	.20	.62	.87	.62	-.05	.04	.64	.81	.60	-.17	.04	.31	.77	.53	-.04	-.13	.36	.76	.64	-.05	.08	.35	.70	.60
9	-.11	-.08	.02	.35	-.04	.04	.39	.73	1.	-.08	-.05	.31	.77	.96	-.12	-.15	.09	.71	.93	-.13	-.23	.18	.83	.92	-.17	-.23	-.04	.81	.90	-.17	-.25	-.11	.58	.90	-.21	-.27	-.17	.35	.84
10	.84	.92	.73	.28	.94	.78	.34	.05	-.08	1.	.91	.41	.03	-.10	.97	.88	.45	.05	-.12	.90	.83	.39	-.01	-.11	.82	.75	.45	.01	-.11	.78	.66	.36	.06	-.08	.63	.51	.24	.06	-.06
11	.83	.89	.82	.46	.93	.90	.56	.25	-.05	.91	1.	.64	.22	-.06	.90	.92	.68	.24	-.09	.81	.83	.59	.12	-.10	.70	.76	.57	.13	-.11	.72	.62	.54	.24	-.04	.61	.58	.44	.28	-.02
12	.44	.48	.63	.64	.52	.73	.87	.74	.31	.41	.64	1.	.76	.34	.42	.60	.86	.75	.29	.33	.49	.85	.61	.27	.21	.49	.68	.61	.22	.36	.31	.70	.74	.36	.36	.51	.66	.77	.38
13	.04	.07	.28	.56	.13	.35	.75	.91	.77	.03	.22	.76	1.	.82	.01	.16	.56	.94	.76	-.05	.05	.64	.92	.74	-.14	.06	.39	.91	.69	-.02	-.06	.38	.87	.79	0	.11	.34	.76	.77
14	-.18	-.13	-.04	.26	-.08	.01	.38	.69	.96	-.10	-.06	.34	.82	1.	-.14	-.16	.10	.75	.97	-.14	-.20	.22	.88	.97	-.16	-.19	.04	.87	.95	-.16	-.21	-.06	.65	.96	-.17	-.22	-.13	.42	.91
15	.86	.93	.76	.30	.94	.80	.35	.05	-.12	.97	.90	.42	.01	-.14	1.	.90	.48	.04	-.17	.92	.86	.42	-.03	-.16	.82	.78	.47	-.02	-.15	.79	.67	.39	.05	-.12	.65	.54	.29	.07	-.11
16	.80	.86	.79	.41	.88	.84	.52	.20	-.15	.88	.92	.60	.16	-.16	.90	1.	.70	.19	-.19	.79	.87	.62	.06	-.19	.67	.78	.58	.06	-.21	.70	.62	.56	.20	-.13	.60	.61	.49	.28	-.10
17	.53	.55	.71	.65	.58	.76	.79	.62	.09	.45	.68	.86	.56	.10	.48	.70	1.	.63	.05	.38	.57	.87	.42	.03	.23	.56	.68	.40	-.04	.40	.33	.74	.59	.12	.38	.56	.72	.69	.14
18	.05	.09	.29	.53	.15	.36	.72	.87	.71	.05	.24	.75	.94	.75	.04	.19	.63	1.	.75	-.02	.09	.66	.90	.71	-.11	.11	.43	.88	.64	.01	-.02	.42	.87	.76	.03	.16	.39	.78	.74
19	-.23	-.16	-.11	.16	-.12	-.05	.31	.62	.93	-.12	-.09	.29	.76	.97	-.17	-.19	.05	.75	1.	-.15	-.21	.18	.86	.97	-.15	-.19	.04	.85	.95	-.16	-.18	-.07	.64	.96	-.16	-.22	-.14	.40	.92
20	.82	.88	.67	.16	.87	.71	.23	-.05	-.13	.90	.81	.33	-.05	-.14	.92	.79	.38	-.02	-.15	1.	.85	.36	-.06	-.14	.93	.83	.49	-.03	-.13	.87	.75	.39	.04	-.10	.74	.60	.28	.05	-.08
21	.74	.81	.67	.21	.81	.74	.37	.04	-.23	.83	.83	.49	.05	-.20	.86	.87	.57	.09	-.21	.85	1.	.57	-.01	-.21	.76	.87	.65	.02	-.21	.78	.72	.56	.16	-.14	.69	.67	.48	.24	-.10
22	.44	.47	.62	.57	.50	.69	.77	.64	.18	.39	.59	.85	.64	.22	.42	.62	.87	.66	.18	.36	.57	1.	.55	.17	.24	.56	.77	.54	.11	.40	.35	.75	.69	.26	.40	.57	.73	.76	.28
23	-.06	0	.15	.41	.05	.22	.60	.81	.83	-.01	.12	.61	.92	.88	-.03	.06	.42	.90	.86	-.06	-.01	.55	1.	.89	-.13	.02	.32	.95	.84	-.05	-.08	.25	.83	.89	-.05	.01	.18	.67	.86
24	-.24	-.16	-.12	.15	-.12	-.06	.28	.60	.92	-.11	-.10	.27	.74	.97	-.16	-.19	.03	.71	.97	-.14	-.21	.17	.89	1.	-.14	-.19	.03	.86	.98	-.16	-.19	-.10	.62	.96	-.17	-.24	-.18	.37	.92
25	.73	.78	.54	0	.77	.58	.10	-.17	-.17	.82	.70	.21	-.14	-.16	.82	.67	.23	-.11	-.15	.93	.76	.24	-.13	-.14	1.	.78	.44	-.08	-.12	.91	.80	.34	-.02	-.11	.77	.59	.22	-.02	-.08
26	.69	.76	.63	.16	.75	.69	.34	.04	-.23	.75	.76	.49	.06	-.19	.78	.78	.56	.11	-.19	.83	.87	.56	.02	-.19	.78	1.	.73	.06	-.20	.81	.79	.64	.22	-.11	.74	.73	.54	.30	-.06
27	.40	.47	.47	.22	.48	.58	.50	.31	-.04	.45	.57	.68	.39	.04	.47	.58	.68	.43	.04	.49	.65	.77	.32	.03	.44	.73	1.	.40	0	.56	.58	.80	.58	.14	.57	.69	.70	.65	.20
28	-.07	.00	.12	.35	.05	.21	.57	.77	.81	.01	.13	.61	.91	.87	-.02	.06	.40	.88	.85	-.03	.02	.54	.95	.86	-.08	.06	.40	1.	.85	0	-.02	.29	.86	.90	.01	.06	.21	.69	.88
29	-.26	-.17	-.16	.08	-.13	-.10	.22	.53	.90	-.11	-.11	.22	.69	.95	-.15	-.21	-.04	.64	.95	-.13	-.21	.11	.84	.98	-.12	-.20	0	.85	1.	-.16	-.18	-.14	.57	.96	-.17	-.26	-.23	.31	.91
30	.76	.79	.63	.13	.78	.67	.25	-.04	-.17	.78	.72	.36	-.02	-.16	.79	.70	.40	.01	-.16	.87	.78	.40	-.05	-.16	.91	.81	.56	.00	-.16	1.	.84	.50	.12	-.11	.85	.74	.40	.16	-.07
31	.58	.63	.45	-.04	.63	.53	.15	-.13	-.25	.66	.62	.31	-.06	-.21	.67	.62	.33	-.02	-.18	.75	.72	.35	-.08	-.19	.80	.79	.58	-.02	-.18	.84	1.	.56	.13	-.12	.76	.74	.43	.18	-.06
32	.42	.44	.52	.35	.45	.61	.57	.36	-.11	.36	.54	.70	.38	-.06	.39	.56	.74	.42	-.07	.39	.56	.75	.25	-.10	.34	.64	.80	.29	-.14	.50	.56	1.	.60	.02	.54	.72	.82	.69	.08
33	.03	.08	.24	.39	.14	.35	.66	.76	.58	.06	.24	.74	.87	.65	.05	.20	.59	.87	.64	.04	.16	.69	.83	.62	-.02	.22	.58	.86	.57	.12	.13	.60	1.	.74	.17	.31	.51	.86	.73
34	-.21	-.13	-.08	.16	-.08	0	.35	.64	.90	-.08	-.04	.36	.79	.96	-.12	-.13	.12	.76	.96	-.10	-.14	.26	.89	.96	-.11	-.11	.14	.90	.96	-.11	-.12	.02	.74	1.	-.11	-.14	-.06	.48	.95
35	.62	.65	.51	.06	.64	.57	.22	-.05	-.21	.63	.61	.36	0	-.17	.65	.60	.38	.03	-.16	.74	.69	.40	-.05	-.17	.77	.74	.57	.01	-.17	.85	.76	.54	.17	-.11	1.	.78	.46	.23	-.05
36	.54	.56	.52	.16	.55	.59	.36	.08	-.27	.51	.58	.51	.11	-.22	.54	.61	.56	.16	-.22	.60	.67	.57	.01	-.24	.59	.73	.69	.06	-.26	.74	.74	.72	.31	-.14	.78	1.	.74	.44	-.08
37	.35	.34	.47	.35	.35	.53	.55	.35	-.17	.24	.44	.66	.34	-.13	.29	.49	.72	.39	-.14	.28	.48	.73	.18	-.18	.22	.54	.70	.21	-.23	.40	.43	.82	.51	-.06	.46	.74	1.	.72	0.
38	.10	.12	.31	.42	.17	.41	.68	.70	.35	.06	.28	.77	.76	.42	.07	.28	.69	.78	.40	.05	.24	.76	.67	.37	-.02	.30	.65	.69	.31	.16	.18	.69	.86	.48	.23	.44	.72	1.	.57
39	-.21	-.12	-.08	.11	-.07	.01	.33	.60	.84	-.06	-.02	.38	.77	.91	-.11	-.10	.14	.74	.92	-.08	-.10	.28	.86	.92	-.08	-.06	.20	.88	.91	-.07	-.06	.08	.73	.95	-.05	-.08	.00	.57	1.

Table 4: *The correlation matrix with systematics' contributions is shown. The bin corresponding to each row or column is shown in figure 11. Trigger and luminosity uncertainty are not reported.*